Time-Lapse High-Resolution Seismic Imaging of a Catastrophic Salt-Dissolution Sinkhole in Central Kansas

by

Jamie L. Lambrecht
B.S., Benedictine College, 2003
Kansas Geological Survey
1930 Constant Avenue
Lawrence, KS 66047-3726

Submitted to the Department of Geology
and the Faculty of the Graduate School of
the University of Kansas in partial
fulfillment of the requirements for the
degree of Master of Science
2006

Thesis Defended April 14, 2006

Kansas Geological Survey
Open-file Report No. 2006-23

Time-Lapse High-Resolution Seismic Imaging of a Catastrophic Salt-Dissolution Sinkhole in Central Kansas

by

Jamie L. Lambrecht
B.S., Benedictine College, 2003

Submitted to the Department of Geology
And the Faculty of the Graduate School of
The University of Kansas in partial
fulfillment of the requirements for the
degree of Master of Science
2006

Advisory Committee:

_____
Richard Miller,
Chair

_____
Don Steeples

_____
Anthony W. Walton

_____
Julian Ivanov

_____
Robert H. Goldstein
for the Department

Date Defended April 14, 2006

The Thesis Committee for Jamie L. Lambrecht certifies
That this is the approved version of the following thesis:

Time-Lapse High-Resolution Seismic Imaging of a
Catastrophic Salt-Dissolution Sinkhole in Central Kansas

Committee:

_____
Richard Miller,
Chair

_____
Don Steeples

_____
Anthony W. Walton

_____
Julian Ivanov

Acknowledgments

I would like to acknowledge the assistance and effort of my thesis committee: Rick Miller who generously shared his knowledge with me, I would not be where I am without his aid; Don Steeples, who kept me going through the revision process; Tony Walton, my first geology professor, who passed on to me his love of geology; and Julian Ivanov who taught me the software and shared his processing knowledge.

I would also like to thank my co-workers: David Laflen whose help was valuable in collecting the multiple data sets; Mary Brohammer who aided in the creation of figures; Brett Bennett whose technical support kept the project up and running; James Dietrich whose DGPS help in ArcView enabled quality figures; Theresa Rademacker whose unrelenting support both technically and emotionally helped me to trudge on; Sally Hayden who helped a grammatically challenged graduate student; Susan Nissen who taught me the Kingdom Suite software used to create the synthetic sweep; and Steve Durrant and Richard Lacey of the Kansas Corporation Commission (KCC) for all the time, help, and information they provided on this project.

Contents

Illustrations

Figures

Tables

Abstract

Time-lapse high-resolution seismic reflection techniques elucidate the subsurface geologic condition of a sinkhole that formed in Pawnee County near the town of Macksville in central Kansas. Collapse of the Macksville sinkhole in 1988 resulted forming a cavity that increased in size with time. This sinkhole is one of a very few that have speculated to form catastrophically from bedded salt dissolution in the central United States. Two orthogonal high-resolution seismic lines were acquired in 1998 and one was acquired in 2005, from a 204-channel fixed spread of geophones. The line acquired in 2005 was kept as close as possible to the equivalent 1998 line. This sinkhole is uncommon in terms of its initial catastrophic subsidence rate and represents a critical data point that with other data may some day allow the prediction of failure prior to surface expression.

Introduction

The Macksville sinkhole (Figure 1) formed catastrophically in July of 1988 around an oil-field brine disposal-well in central Kansas (T23S, R15W, Sec. 30, SW) (Figure 2). Most sinkholes in central Kansas form as a result of dissolution of the Permian Hutchinson Salt Member (Miller et al., 1993; Miller et al., 1997) (Figure 3). Since 1979 the Kansas Geological Survey has studied numerous sinkholes using high-resolution seismic-reflection techniques in an attempt to better understand the mechanisms that control their formation (Miller et al., 1997).

Sinkholes are a hazard to property and human safety in various geologic settings (Parker, 1967; Lohmann, 1974; Anderson and Kirkland, 1980; Beck 1984; Nieto et al., 1985; Miller et al., 1993; Ge and Jackson, 1998; Cartwright et al., 2001). Surface subsidence can progress at a range of rates depending on site-specific geologic and hydrologic settings (Miller et al., 1997; Samuel and Trader, 2002; Lambrecht and Miller, 2006). A sinkhole's subsidence rate, which can range from gradual to catastrophic, correlates to its risk to public safety and property damage (Miller et al., 1990).

Shallow high-resolution seismic-reflection techniques have been successful at defining stratigraphic and structural features associated with several salt dissolution features in Kansas (Steeples, 1980; Steeples and Knapp, 1982; Steeples et al., 1983; Miller et al., 1985; Miller et al., 1988; Miller et al., 1990; Miller et al., 1993; Miller et al., 2002; Miller, 2003; Lambrecht et al., 2004a; Miller et al., in press). Prominent high-amplitude seismic reflections from shallow Permian redbed sequences, the Stone

Figure 1: A photo taken looking toward the southeast during the 1998 survey.

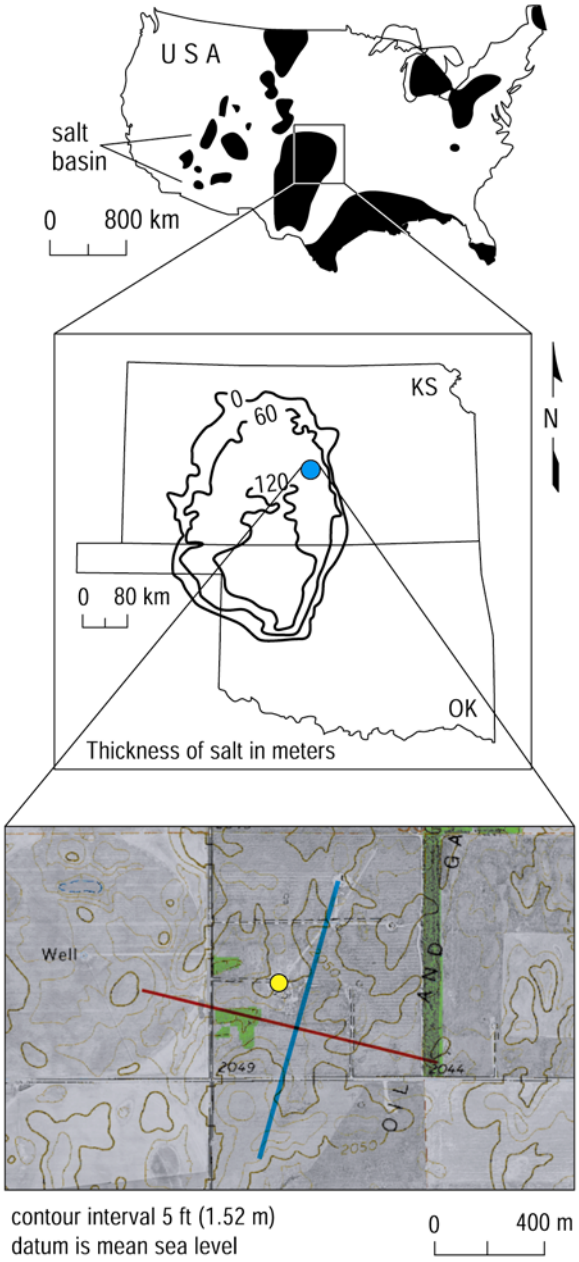

Figure 1: (top) Site map relative to bedded salt deposits, shown darkly shaded (modified from the Salt Institute, 2003). (middle) The Hutchinson Salt is a bedded salt deposit that extends from central Oklahoma across most of south-central Kansas (Modified from Walters, 1978). (bottom) Two 1-km seismic profiles superimposed on topography and orthophotos, Pawnee County, Kansas. The yellow dot is the approximate location of the Macksville sinkhole, the red line is the approximate placement of the 1998 and 2005 west-east surveys, and the blue line is the approximate placement of the north-south line from the 1998 survey.

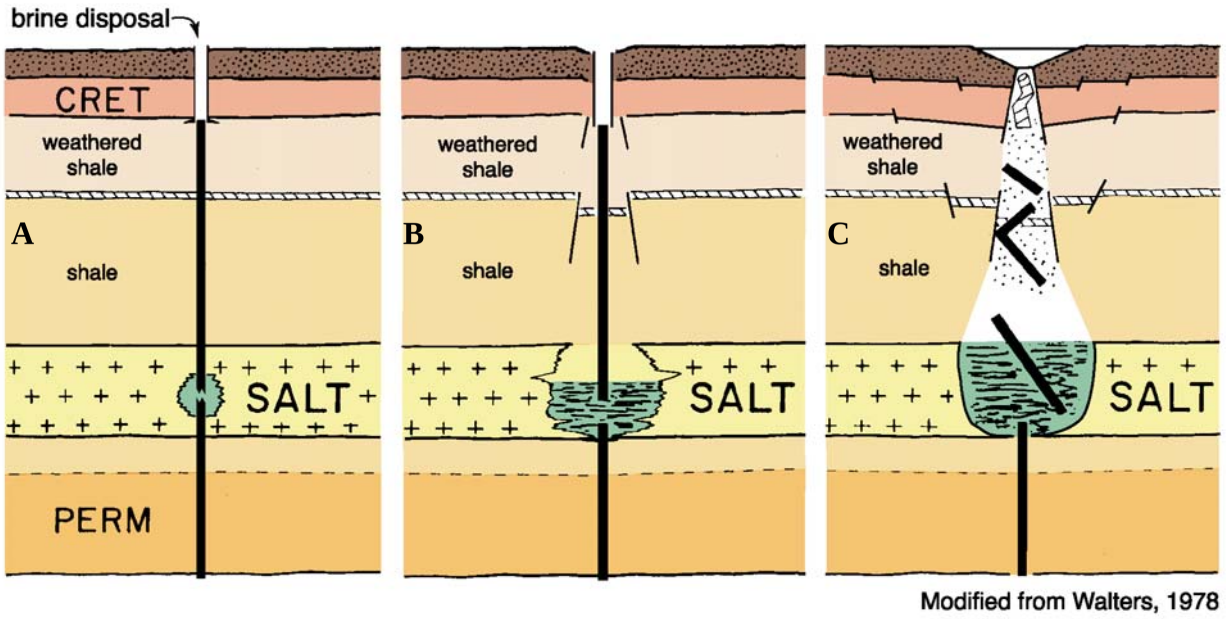

Figure 2: The horizontal growth of a sinkhole controlled by normal faults. A) A small leak within a brine-disposal well. Stress builds up within the tensional dome. B) Dissolution of salt by brine water creates the steep-sided chimney structure. C) Enlargement forms an open bowl.

Corral Anhydrite, and anhydrites and shales within the Hutchinson Salt Member provide an image of the subsurface. Data quality has hindered an association of the subsurface to the surface.

Advancements in near-surface seismic methods over the past 25 years have significantly improved the resolution potential and the diversity of problems that can be studied seismically (Corüh and Costain, 1983; Hunter et al., 1984; Knapp and Steeples, 1986a; Knapp and Steeples, 1986b; Miller, 1992; Doll and Corüh, 1995; Baker et al., 1998; Allen et al., 1998; Ivanov et al., 1998). The addition of more channels into a seismic record has permitted closer geophone spacing and therefore more traces within the optimum window (Hunter et al., 1984). Any increase in the signal-to-noise ratio allows for a more detailed interpretation of the final stacked seismic section.

Site-by-site defining of the collapse and its effect on rock layers between the salt and ground surface helps build an experienced-based approach to estimating the potential threat of sinkholes. Also, by evaluating the subsurface an appropriate remediation plan can be developed that will reduce or possibly eliminate the threat to surface activities a specific sinkhole can represent.

Overburden slumping has been identified as a sign of dissolution failure (Knapp, 1989) and associating sinkhole formation with the tensional dome defining the lines of stress (Villella, 1998), our understanding of sinkholes is getting closer to prediction of their future course. The time-lapse study of the Macksville sinkhole provides an understanding of one aspect of this sinkhole's formation that with future

studies will one day enable enhanced prediction of future failure prior to surface expression of subsurface salt dissolution.

Geologic Background of Pawnee County, Kansas

Permian rocks in Kansas are predominantly marine deposits in the lower section (Chase Group, Sumner Group) becoming non-marine deposits in the upper section (Nippewalla Group) (Zeller, 1968). These rocks have a prevailing west to northwest dip of about a meter for every kilometer traveled (Merriam, 1963). For this study, most rocks within the depth range of interest are lower Permian (Figure 4), but the overburden rocks have an affect on the seismic signal. The shear strength of the Permian rocks is greatest for limestone and least for halite with anhydrite and shale falling in between respectively (Handin, 1966).

The oldest group of interest for this survey is the Chase Group. Within Pawnee County, this group is made up of roughly 100 m of alternating limestone and red and green shale (Zeller, 1968). The overlying Sumner Group contains the Wellington Formation, Ninnescah Shale, and the Stone Corral Formation. The Wellington Formation includes 200 m of marine to freshwater deposits (Merriam, 1963) and the Hutchinson Salt Member, the focus of this study. The Runnymede Sandstone Member marks the top of the Ninnescah Shale and is a very fine-grained siltstone to sandstone with a thickness approximately 2.3 m (Zeller, 1968). For the most part, the rest of the Ninnescah Shale is predominantly silty shale but containing some limestone, dolomite, and calcareous siltstone (Zeller, 1968). The Stone Corral Formation is composed of dolomite, anhydrite, gypsum, and salt and consists of two massive anhydrite beds separated by a shale bed with a total thickness of approximately 7.5 m to 13.5 m (Merriam, 1963).

System	Series	Group	Formation or Member		General Character of Rocks
PERMIAN	Lower Permian	Nippewalla Group	Cedar Hills Ss.		Red feldspathic sandstone, siltstone, and shale
			Salt Plain Ss.		Red siltstone and shale
			Harper Ss.		Red argillaceous siltstone and sandstone
		Sumner Group	Stone Corral		Dolomite and anhydrite
			Ninnescah Sh.	Runnymede Ss. Mbr.	Gray siltstone and sandstone
					Reddish brown shale and siltstone
			Wellington Formation	"Upper Member"	Dark gray shale
				Hutchinson Salt Member	Salt with interbedded anhydrite, shale, magnesite, and dolomite
				"Lower Member"	Anhydrite and gray shale with interbedded dolomite
		Chase Group			Limestone, dolomite, and variegated shale beds

Figure 4: Simplified stratigraphic chart for area of interest (modified from Villella, 1998; Zeller, 1968).

The Nippewalla Group is commonly referred to as the redbed sequence because they are predominantly red in color due to the presence of ferric oxide (hematite) usually coating individual grains (Zeller, 1968). This group consists of the Harper Sandstone (approximate thickness 65 m), the Salt Plain Formation (approximate thickness 80 m), and the Cedar Hills Sandstone (approximate thickness 54 m) (Zeller, 1968). Generally, these consist of a predominantly thick sequence of redbeds that during deposition formed a nearly featureless plain (Zeller, 1968). A variety of rocks makes up this group including silty shale, siltstone, very fine-grained sandstone, and dolomite (Merriam, 1963). In other areas of Kansas this group also contains evaporite layers. The Cedar Hills sandstone is extremely porous (Merriam, 1963) and was used as a shallow disposal zone for oil field brines until the mid-1940s when contamination of this aquifer became evident (Jones, 1945).

Overburden rocks of the Cretaceous, Tertiary, and Quaternary, while not within the stratigraphic section of interest, can still affect the seismic data. The lowest Cretaceous members contain sandstone with increasing shale content moving up in the section (Kiowa Formations; Zeller, 1968). The upper Cretaceous is shale with thin limestone beds (Greenhorn Limestone, Carlile Shale, Niobrara Chalk, and Pierre Shale; Zeller, 1968). The Tertiary and Quaternary systems contain sand, gravel, silt, and clay. This unconsolidated material would attenuate the seismic signal therefore decreasing resolution of the common midpoint stacked section. There is a predominant confined ground-water flow in the Quaternary sediments towards the east-northeast (Whittemore, 1989).

Evaporite Deposits

Several major salt basins exist in North America (Figure 2; Ege, 1984). The Permian Hutchinson Salt Member, which underlies a significant portion of south-central and central Kansas (Figure 2), formed in one such basin. This member is present in the subsurface across some 37,000 mi^2 (95,830 km^2) in Kansas and represents a subsurface volume of approximately 1,100 mi^3 (4,585 km^3) (Watney, 1988). Average net thickness of the Hutchinson Salt Member in Kansas is 76 m, but it reaches a maximum of over 150 m in the southern part of the basin (Zeller, 1968).

The Hutchinson Salt Member is composed of many separate halite beds ranging from 0.15 to 3 m thick and interbedded with shale, minor anhydrite, and dolomite (Watney, 1988). This bedded salt is the remnant of a shallow land-locked Permian sea, which intermittently was open to recharge with brackish ocean waters from the south. The anhydrite beds in the halite section have a strong seismic signature and are locally continuous but regionally discontinuous. In this study area the halite interval is 125 m thick. The halite-rich interval is the key to time-lapse interpretation and associated speculation about the growth process of the sinkhole.

There are two reasons the halite beds are still intact over 250 million years after their deposition. First, the Hutchinson Salt member is located in a tectonically quiet area and, with the exception of the edges, is relatively flat lying (Merriam, 1963). At the edges extreme distortion occurs in some locations due to localized exposure to the natural infiltration of groundwater (Figure 5). Second, most of the Permian rock overlying the salt bed is shale (Zeller, 1968). These shales are

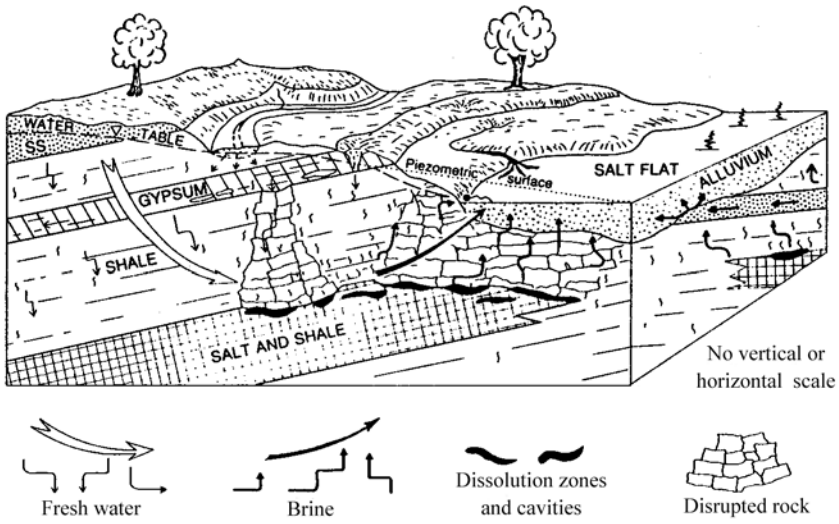

Figure 5: Depiction of the dissolution front for interstratal salt karst in western Oklahoma (Johnson, 2005). A similar dissolution front is located in central Kansas approximately 40 km east of survey site

over 100 m and have protected the salt by maintaining a very low permeability to the relatively fresh groundwater present in several Permian, Cretaceous, Tertiary, and Quaternary aquifers.

Seismic Aspects

The seismic-reflection method detects changes in subsurface material properties (Table 1). Lateral changes in the acoustic impedance of subsurface layers and features can indicate changes in the subsurface (Sheriff, 2002). Materials with larger acoustic impedance overlying materials with smaller acoustic impedance will result in a negative reflectivity (Yilmaz, 2001). Wavelet polarity follows reflection coefficients that are negative when faster or denser layers overlie slower or less dense layers and positive when slower or less dense layers overlie faster or denser layers. The Stone Corral Formation is one such case with a shale bed encased by two anhydrite beds and makes this formation a seismic marker bed throughout central and western Kansas.

The bed thickness visible in seismic-reflection studies depends on the frequency of the waveform and seismic velocities; higher frequencies will image thinner beds. Higher frequencies are attenuated with depth (Yilmaz, 2001) therefore with depth there is a decrease in resolution of beds. At the Macksville site bed resolution declines from approximately 6 m at the depth of the Stone Corral Formation to approximately 18 m within the Hutchinson Salt Member (Table 2). The horizontal resolution ($R=((D\lambda)/2)^{1/2}$ where R=resolution, D=depth, λ=wavelength) and of the data is 150 meters therefore the internal features of the units cannot be mapped.

Material	P-wave Velocity (m/s)	Density (kg/m^3)	Acoustic Impedance (kg/m^2s)*
Dry sand/gravel	750	1800	$1.35 * 10^6$
Clay	900	2000	$1.80 * 10^6$
Saturated sand	1500	2100	$3.15 * 10^6$
Saturated clay	1800	2200	$3.96 * 10^6$
Shale	3500	2500	$8.75 * 10^6$
Sandstone	2850	2100	$5.99 * 10^6$
Limestone	4000	2600	$10.4 * 10^6$
Anhydrite	4100	2900	$11.89 * 10^6$
Halite**	5500	2200	$12.1 * 10^6$

Velocities are mean for a range appropriate for the material.
*Acoustic impedance is velocity multiplied by density, specifically for compressional waves.
** Velocity and density will decrease when water is within the halite.

Table 1: Approximate material properties (modified from ASTM Guide D 7128 – 05; and Carmichael, 1989).

Material	Representative P-wave Velocity (m/s)	Frequency (Hz)	Theoretical ¼ λ (m)	Practical ½ λ (m)
Dry sand	500	50	2.5	5.0
		100	1.25	2.5
		200	0.62	1.25
	1000	50	5.0	10.0
		100	2.5	5.0
		200	1.25	2.5
Wet Sand/Dry Clay	1500	50	7.5	15.0
		100	3.75	7.5
		250	1.5	3.0
Tight, Wet Clay/Shale	2000	50	10.0	20.0
		100	5.0	10.0
		250	2.0	4.0
Shale	2500	50	12.0	25.0
		100	6.25	12.5
		250	2.5	5.0
Shale/Sandstone	3000	50	15.0	30.0
		100	7.5	15.0
		250	3.0	6.0
Sandstone/Limestone	3500	50	17.5	35.0
		100	8.75	17.5
		250	3.5	7.0
Limestone	4000	50	20.0	40.0
		100	10.0	20.0
		250	4.0	8.0
Anhydrite	4100	50	20.5	41.0
		100	10.25	20.5
		250	4.1	8.2
Halite	5500	50	27.5	55
		100	13.75	27.2
		250	5.5	11

Table 2: Vertical layer resolution limits (λ=F/V (where λ=wavelength, F=Frequency, V=P-wave velocity) (modified from ASTM Guide D 7128 – 05).

Formation of Sinkholes Due to the Salt Dissolution Processes

Rock salt has the highest solubility of common rocks (Carmichael, 1989). Solubility of gypsum and halite are 150 and 7,500 times, respectively, more soluble than the average limestone (Martinez et al., 1998). The solubility of halite in groundwater is 35.5% by weight at 25 ^{o}C, with increasing solubility at higher temperatures (Martinez et al., 1998). Halite goes into solution by dissolution and not by chemical reactions. The amount of halite removed from a system is controlled by the equilibrium of solubility between rock salt and the water flowing through it (White, 1988).

Four basic requirements are necessary for the dissolution of an evaporite (Johnson, 2005):

1) An evaporite deposit through which water can flow.
2) A supply of water unsaturated relative to halite or gypsum concentrations.
3) An outlet whereby the brine can escape.
4) Energy, such as hydrostatic head or density gradient, to cause the flow of water through the system.

Dissolution can occur when under-saturated groundwater moves through and comes into contact with subsurface salt beds. The dissolution process can be continuous as long as unsaturated fluids are in contact with the salt beds. Substantial dissolution occurs when a conduit system provides a continuous source of mobile unsaturated

brines to contact salt and a mechanism for saturated brines to exit the active dissolution area.

Both deliberate and inadvertent dissolution of the Hutchinson Salt Member has occurred as a result of anthropogenic activity. Engineered dissolution for mining involves a one-well or two-well system providing the inlet for fresh water and outlet for brackish fluids (Johnson, 2005). Many of the dissolution voids left by this process are used for liquefied petroleum gas (LPG) storage after production of salt has concluded. The few documented cases of anthropogenic dissolution of the Hutchinson Salt Member that have culminated in sinkhole formation ensued from petroleum activities. Most of the petroleum production-associated sinkholes can be attributed to practices used before the development of proper engineering safe guards in drilling-mud design, casing placement, and salt tolerant cements (Johnson, 2005).

Subsidence Due to Oil and Gas Activities in Kansas

In 1978 there were only eight confirmed cases of land subsidence that could be attributed to oil and gas operation out of the 80,000 oil and gas test holes drilled through the Hutchinson Salt Member at that time in Kansas (Walters, 1978). This yields a ratio of onsite of land-subsidence occurring for every 10,000 oil and gas test holes. In each of these cases subsidence was associated with a brine-disposal well.

Oil field brines were disposed in shallow salt-water wells beginning in the 1940s (Jones, 1945). Prior to that the brine wastewater was disposed of in surface ponds where the water evaporated and the salt residue was left behind. Due to the lack of an impermeable seal on these evaporation ponds or to poor construction,

brackish fluids routinely mixed with local groundwater or streams (Jones, 1945). Disposal wells initially injected brine into brackish aquifers above the Hutchinson Salt Member, but this quickly led to contamination problems. This approach, for the most part, was abandoned in the 1950s, when deep Arbuckle salt-water disposal systems became the accepted solution to the oil field brine problem (Walters, 1991).

When a disposal well penetrates the impermeable shales separating surface and fresh water aquifers from the salt, casing integrity and formation grouting must be maintained to avoid Johnson's (2005) number 2, 3, and 4 of the criteria necessary for subsidence. If either the casing or the grout seal fails, a continuous pathway develops for unsaturated water to access the salt, and dissolution can commence (Figure 3). The process will not stop until one of the four criteria is no longer met. Formations located above the Hutchinson Salt member, such as the Cretaceous Cheyenne Sandstone and the Permian Cedar Hills Sandstone, are saturated with slightly brackish water and can significantly affect the dissolution process once a pathway exists. State regulations for fresh water aquifers, such as being isolated from the production casing by surface casing (Walters, 1978) do not apply to these brackish aquifers.

At an early stage in their formation, disposal-well induced sinkholes usually appear centered on the well bore; this is solid evidence for suggesting dissolution is due to under-saturated brines accessing the salt through corroded casing, (Knapp et al., 1989) or insufficient cement seal in the annular space. Cementing casing opposite

fresh water zones is a practice adopted by the industry early on and has been required since 1935 by state regulations (Walters, 1978).

Brines from the Arbuckle Group are under-saturated as to sodium chloride and characteristically contain H_2S, which is corrosive to metals. Arbuckle Formation brine water has as much as six times the chloride concentration of seawater (20,000 ppm; Jones, 1945). If a well has a corroded or faulty casing, even Arbuckle brines that are injected could allow for the uncontrolled dissolution of salt.

Macksville Sinkhole Chronology

Farmland co-exists with operations at the Benson Oil and Gas Field in southeastern Pawnee County, Kansas. Several abandoned wells in this area had previously been injecting brackish reservoir waste fluids into the 1.5 km deep Arbuckle Formation. One of these disposal wells, the Garvin 4 (API 15-145-01061) operated by M.B. Armer Drlg Co. and plugged in 1984, had been remediated sufficiently to allow continuous surface farm operations directly over the old well location.

On July 21, 1988, a farmer was tilling one of his fields in the Benson Oil and Gas Field After moving to another nearby field the farmer observed a substantial cloud of dust rising from the field, he had just left. The curious farmer returned to investigate and discovered a sinkhole tens of meters deep with nearly vertical sides and a throat several meters wide. Water was cascading into this chimney feature from the walls some distance below ground surface. In the eighteen years since this catastrophic collapse, nearly continuous gradual subsidence has enlarged the sinkhole to include a total area affected of more than 40,000 m^2 (Figure 6).

Concern for the Great Bend Prairie aquifer, which is used in the area for irrigation and the watering of stock, caused the KCC to install four observation wells in 1989 at the base of the aquifer around this sinkhole. Ground water sampled from these wells was determined to be saline on the east and northeast sides of the sinkhole but fresh to the southwest (Whittemore, 1989). Immediate concern was for a well

used for irrigation within a quarter mile of the salt-water plume as well as two other irrigation wells approximately a half-mile from the plume (Whittemore, 1989).

Figure 6: Panoramic photograph of the Macksville Sinkhole looking to the northeast taken during the 2005 survey.

A geochemical analysis of the water in the sinkhole was conducted to determine origin and to formulate a potential flow model (Whittemore, 1989). A water sample taken from the sinkhole possessed a chloride concentration of 35,000-37,500 mg/L and was from a halite solution chemically similar to seawater (Whittemore, 1989). This same solution was found in the contamination plume, which contained less than 2% oil field brines (Whittemore, 1989). The water table in this area is 6 to 9 meters below the surface. Predominant ground-water flow in the Quaternary sediments was toward the east-northeast with one-third of the plume advancing in that direction (Whittemore, 1989). This groundwater study indicates communication between the aquifers and the salt in proximity to this sinkhole thereby establishing a virtually endless fresh water source.

Method

Seismic Acquisition at the Macksville Sinkhole

In 1998 seismic reflection data were acquired along two fixed 204-station, 1 km spreads, one north-northwest to east-southeast, the other north-northeast to south-southwest, in Pawnee County, Kansas (T23S, R15W, Sec. 30, SW). They were designed to image the dissolution-affected subsurface optimally (Figure 2). In 2005 a repeat west-east line was acquired (Figure 7) to both evaluate the effectiveness of time-lapse seismic surveys as a tool for monitoring salt dissolution sinkholes and to evaluate the subsurface growth and changes relative to surface expansion over the seven-year period between 1998 and 2005.

Data acquired for the 2005 monitor survey were as comparable as possible with respect to 1998 legacy data. Three 40 Hz geophones for the 1998 survey and two 40 Hz geophones for the 2005 survey were seated into the sandy soil at 5 m intervals; this was the source spacing as well. An IVI Minivib I (Figure 8) generated four 10-second, 30-250 Hz up-sweeps at each shot station; each shot gather was recorded individually by a 240-channel, 24-bit, networked Geometrics StrataView seismograph system (four, 60 channel units; Figure 9). Data from each of the four sweeps at each shot station were recorded and stored as uncorrelated files along with the ground force pilot. These uncorrelated field records were evaluated to determine a suitable processing approach (Lambrecht et al., 2004b). The first sweep at each station was intended to seat the base-plate and was not included during processing of the

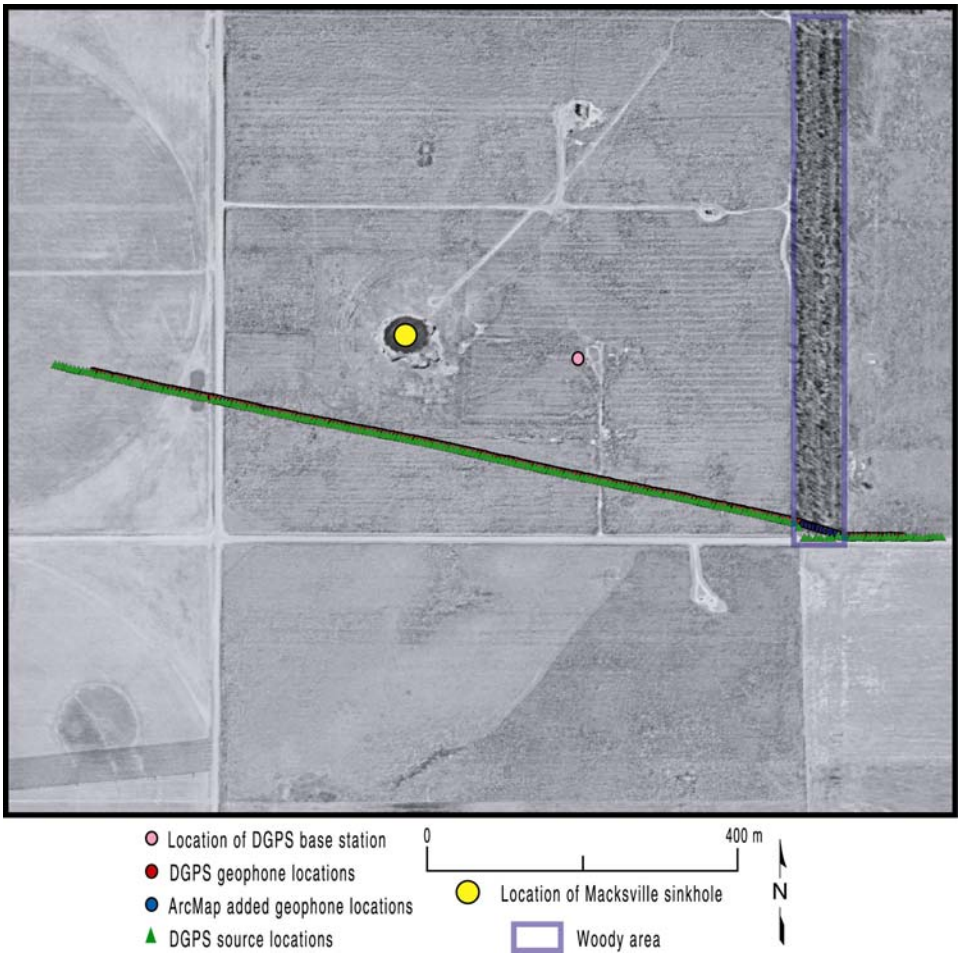

Figure 7: DGPS source and receiver locations of the 2005 seismic line.

Figure 8: Photograph of the IVI Minivib I.

Figure 9: Photograph of the seismograph setup.

common-midpoint (CMP) stacked sections. Data were recorded at night for both surveys to minimize environmental noise (predominantly wind noise).

An elevation survey was conducted at the end of each survey. For the 1998 survey, geospatial data were acquired using a hand level, a measuring rod, and topographic maps: unfortunately these data lacked the resolution potential necessary for exact line re-deployment. In the 2005 survey, a differential global positioning system (DGPS) recorded the elevations of each geophone and source location (Figure 7). This detail on the 2005 survey proved extremely useful in building the spread geometries for processing. A large line of trees, approximately 45 m wide, prevented the DGPS from finding the true position of nine geophones due to a lack of satellite contact. Given that geophone spacing was known, these missing DGPS locations were supplemented into ArcMap at a later date (Figure 10). DGPS allowed quality control checks on the true location of the source around this woody area. Three source stations were skipped during the 2005 survey and their locations were not accurately known. The DGPS source and geophone locations were scrutinized in ArcMap (Figure 10), which enabled accurate sort geometry to be defined.

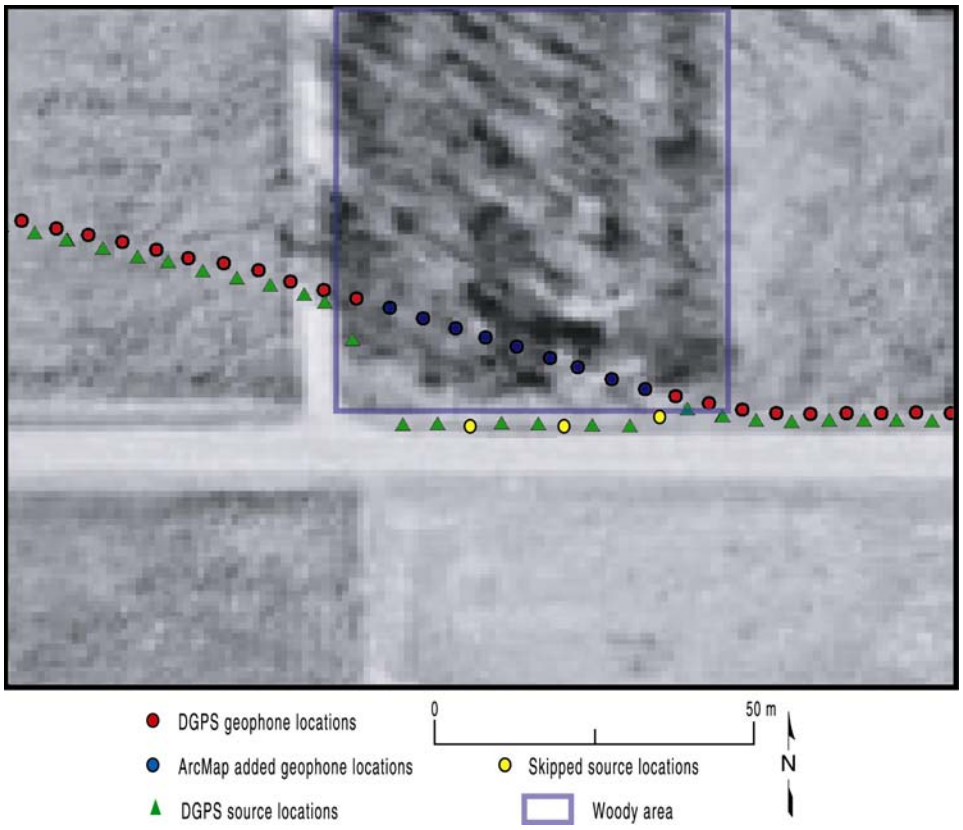

Figure 10: Detail view of wooded area on the east end of the 2005 survey.

Seismic Processing of the Macksville Sinkhole Data

Seismic data were processed using a common-midpoint (CMP) approach generally consistent with those routinely used for high-resolution vibroseis data (Figure 11). Software (WinSeis 2) used was appropriate for processing 2-D high-resolution seismic-reflection data (Steeples and Miller, 1990). Data were plagued with massive static problems as a result of highly disturbed near-surface layers associated with subsidence (surface fissures were up to a meter wide and deep). There was an approximately 10 msec shift noted in reflections without static processing techniques and a 3 msec in reflections with static processing applied to the data. These static problems have their origin in near-surface velocity and surface elevation variability across minimal interval distances along the entire profile where subsidence is evident. Pre-correlation processing focused on the retention and enhancement of higher frequencies and this optimized the signal-to-noise ratio.

A recorded trace for vibroseis data results from a swept source function convolved with the reflectivity series of the earth. When the sweep function is correlated with the recorded data the remaining trace should equate to the reflectivity series convolved with a Klauder wavelet. The synthetic sweep was cross-correlated with the recorded signal traces to produce the reflectivity series convolved with a band-limited zero-phase Klauder wavelet (Yilmaz, 2001). Problems with this method include:

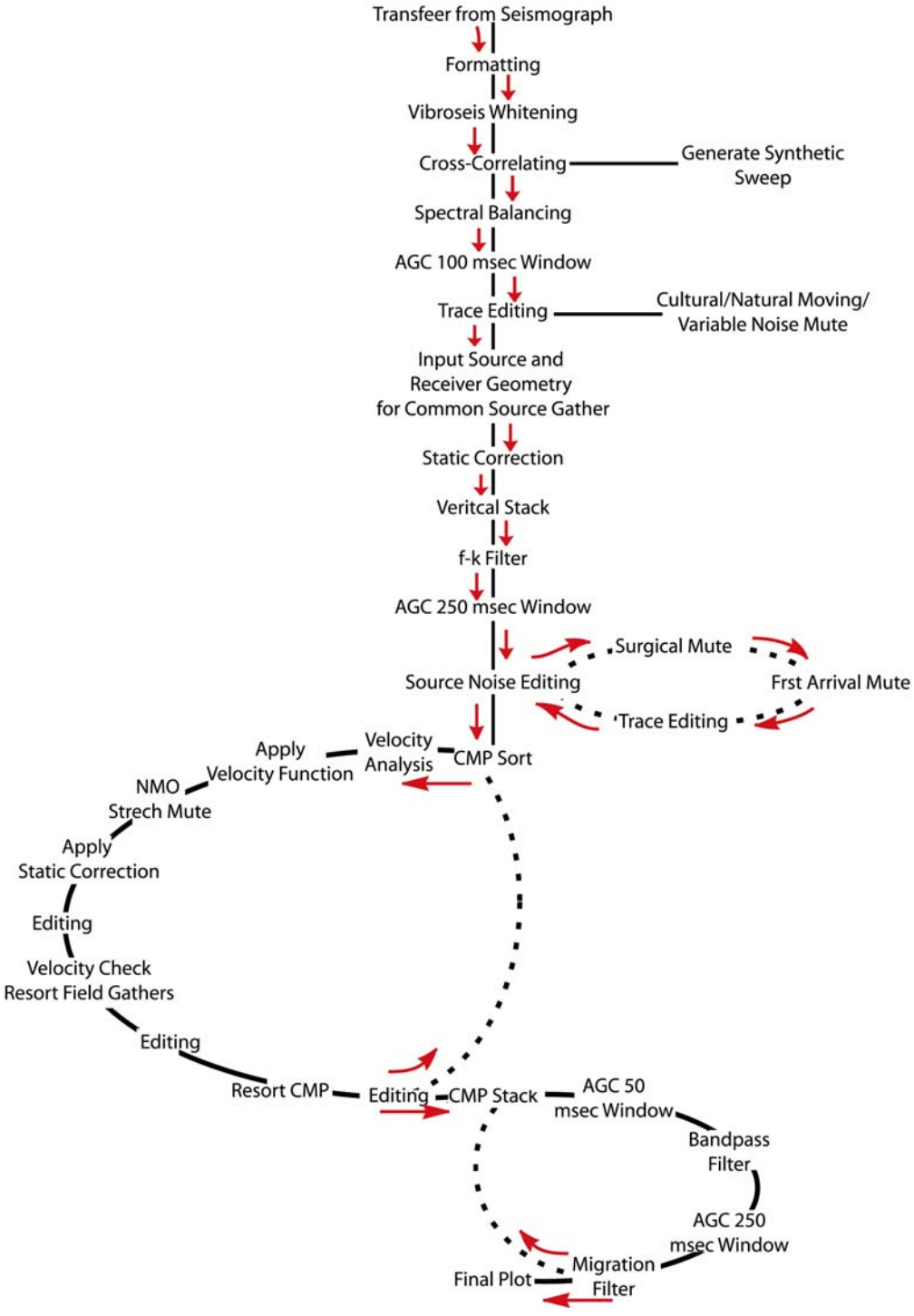

Figure 11: Standard 2-D high-resolution near-surface seismic-reflection processing flow (modified from Miller and Steeples, 1991).

1) Lack of compensation for changes in amplitude and phase due to linear and non-linear filter effects from the vibrator system and base-plate earth coupling.
2) 'Earth filtering' affects the waves as they propagate through the rock.

The result is degradation of the higher frequencies more rapidly than the lower frequencies with offset (Brittle et al., 2001).

Vibroseis whitening is a process based on the application of time-varying amplitude scaling before crosscorrelation (Carüh and Costain, 1983), which can help compensate for reduced amplitudes within the recorded spectra. Near-surface high-resolution seismic-reflection data can be overwhelmed with high ambient noise and suffer seriously from very low signal levels. This is especially true within the higher frequency portion of the useable bandwidth, reducing the resolution potential of recorded data (Doll and Carüh, 1995). Vibroseis whitening enriches the data bandwidth and thereby improves the apparent coherency and resolution potential of near-surface reflections (Klemperer, 1987) easily hidden by the low-frequency narrow-bandwidth ground roll (Figure 12). Spectral characteristics were improved and the signal-to-noise ratio was increased on data from this study as a direct result of using Vibroseis whitening (Lambrecht et al., 2004b). Most near-surface high-resolution seismic-reflection surveys benefit from spectral enhancements or balancing (Doll et al., 1998). Enhancing the high-end portion of the reflection bandwidth and increasing the signal-to-noise ratio is usually a benefit.

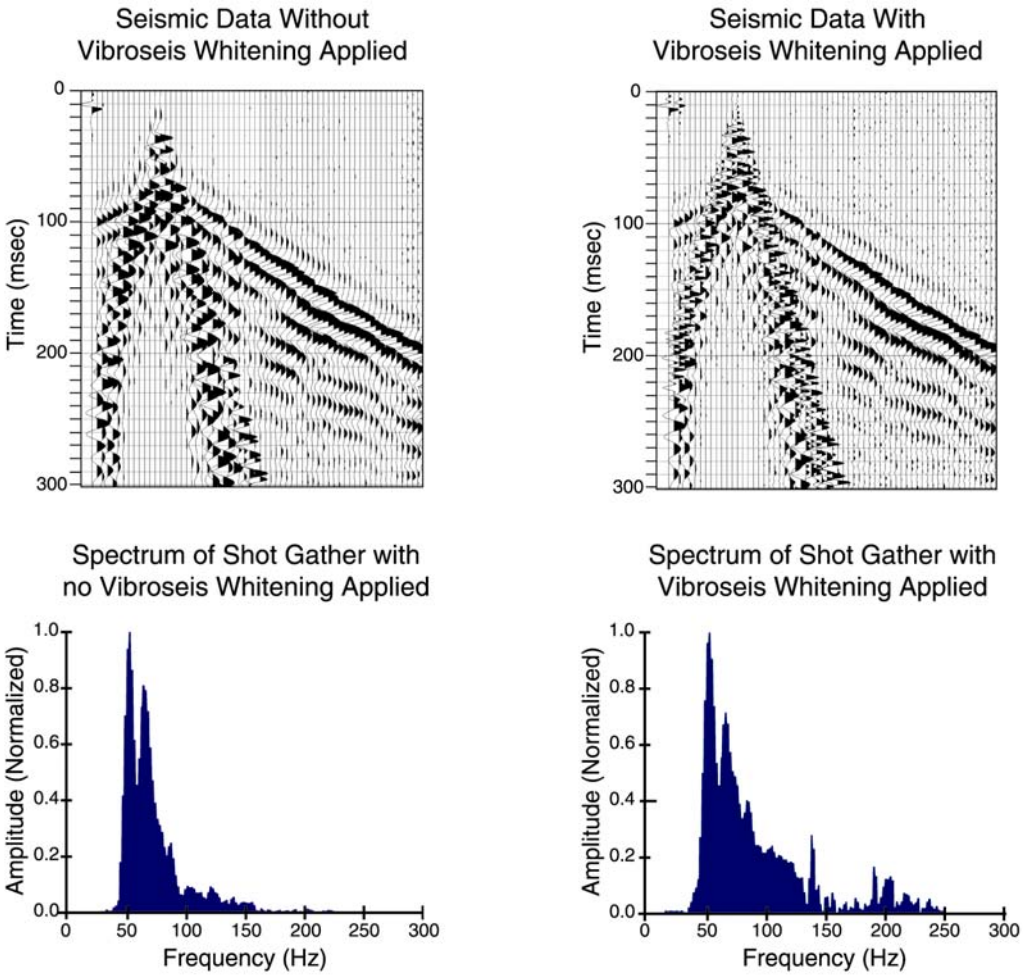

Figure 12: Pre-correlation without Vibroseis whitening applied compared to Vibroseis whitening pre-correlation. Only the first 60 traces were looked at.

Shot Domain Processing

The data were collected in SEG2 format and converted to the comma-delimited KGS format. For the 1998 survey the seismographs were run using a master-slave configuration requiring the data to be merged from the four individual seismic files (each output by a different seismograph) containing 60 channels each, to one file containing 240 channels. For the 2005 survey the data were stored natively as 240-channel records.

Data were cross-correlated with a synthetic sweep after the signal-to-noise improvement with the application of Vibroseis whitening. A synthetic seismic trace was produced that matched the vibrator's drive signal. A linear upsweep, like the one used to produce these data, is a continuously oscillating constant amplitude signal whose instantaneous frequency varies monotonically with time (Goupillaud, 1976). This is often referred to as the ideal theoretical drive and is not a perfect match to what the MiniVib I actually imparts into the ground. Ideally deconvolution would yield better reflections and improved resolution. At this time we are unable to determine if the ground force measured by the accelerometers on the reaction-mass base-plate system computes what is going into the ground.

Automatic gain control (AGC) simulates feedback normalization by applying a variable gain factor to each of the individual samples based on the average amplitude of the surrounding data within the assigned window (Sheriff, 2002). The start time could be manually controlled to allow the AGC to skip the early, high amplitude, first break arrivals. At this point in the processing flow an AGC was

applied with a 250 msec window and a start time of zero. A band-limiting spiking deconvolution, referred to as spectral balancing, was applied after the AGC.

A static time adjustment was applied to each of the four individually recorded sweeps at a shot station to improve the vertical stacking of the data. Source and receiver geometry were defined for each shot record acquired at each vibration point (vp). Once common shot gathers were vertically stacked, a narrow-slice F-K filter was applied targeting the first arrivals. This process simply employs a velocity filter in the frequency-wave number domain. This process was used to reduce first-arrival noise and improve the signal-to-noise ratio in the early part of the gather. Muting of these data was designed to reduce first arrivals, air coupled waves, and ground roll. At this point the noise was minimized as much as practical using a reasonably straightforward approach.

Common-Midpoint Domain Processing

Data quality was evaluated after sorting into CMP gathers (Figure 13). Noisy traces were muted. Velocity analysis (Figure 14, 15, and 16) and normal moveout (NMO) corrections were applied (Figure 17). After NMO corrections data were resorted into shot gathers as an additional quality control step. This display format enabled visual appraisal of effectiveness of "flattening" accomplished by the designated velocity function. Data were then resorted to CMP gathers and stacked to produce a continuous 2-D section.

A 50 ms AGC band pass filter and one last 250 ms AGC were applied to equalized amplitudes and to assist in interpretation. An F-K migration filter proved

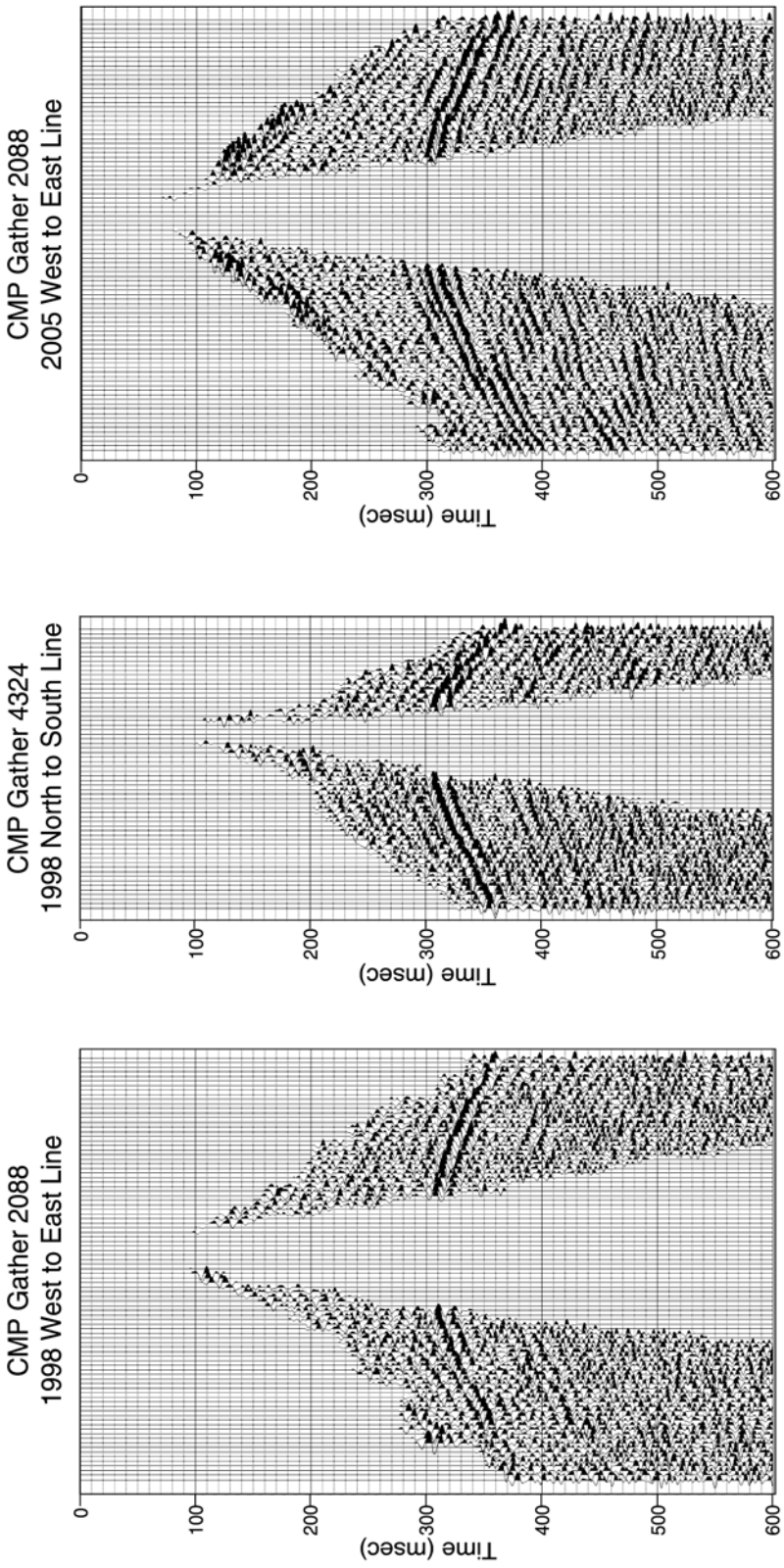

Figure 13: CMP gathers with muting and trace editing already applied.

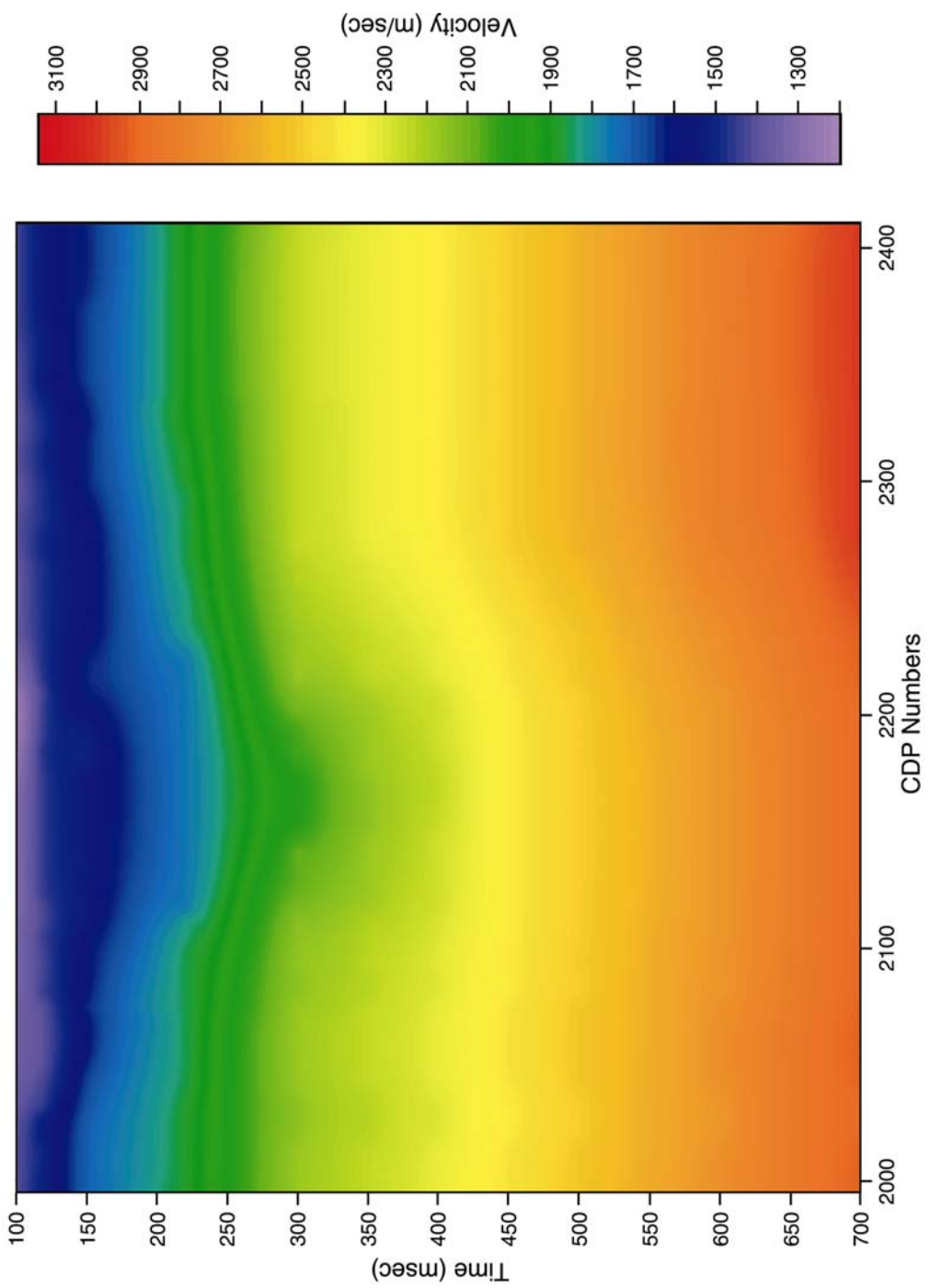

Figure 14: 1998 west-east velocity model used in the NMO correction during the processing flow.

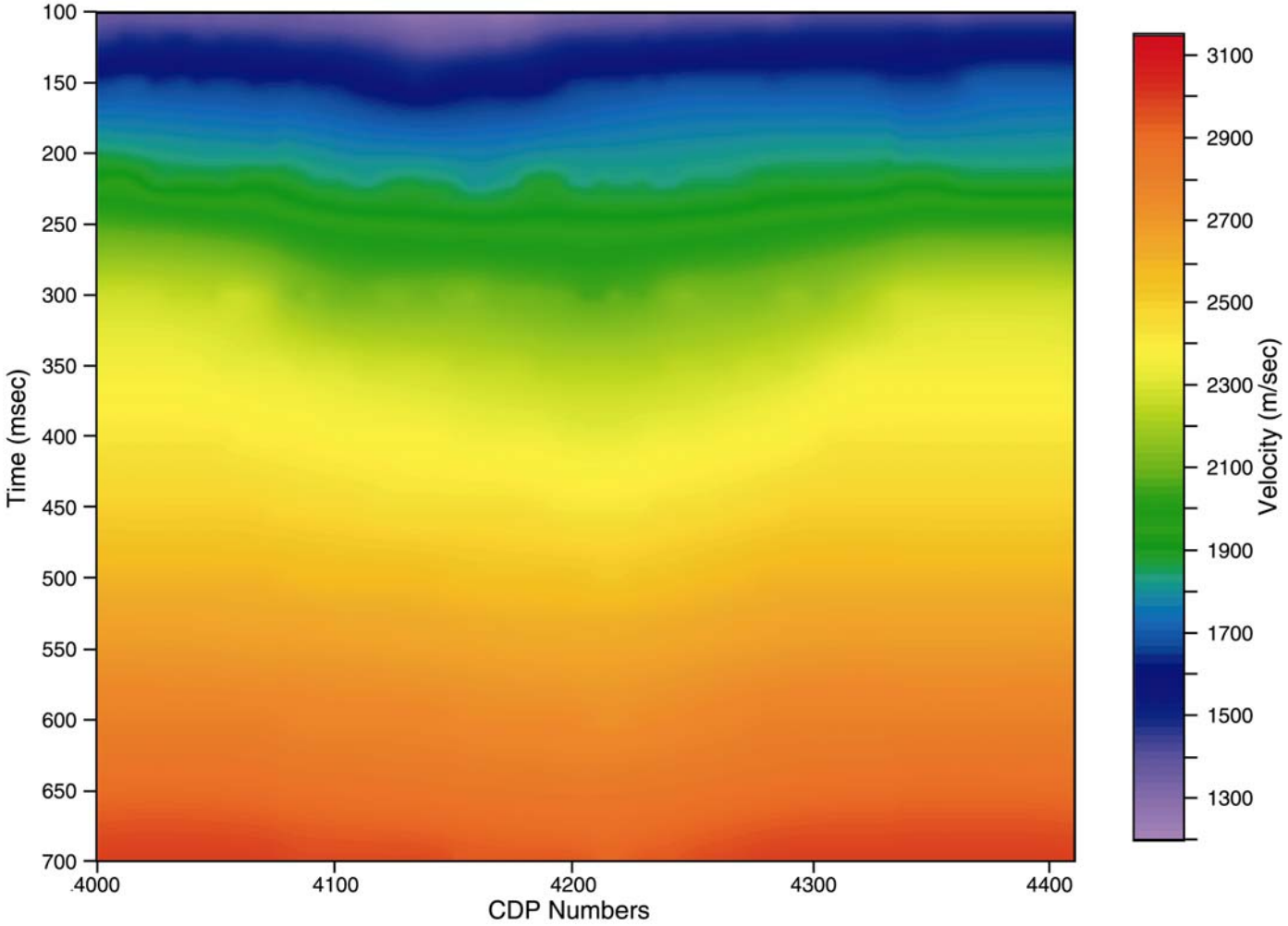

Figure 15: 1998 north-south velocity model used in the NMO correction during the processing flow.

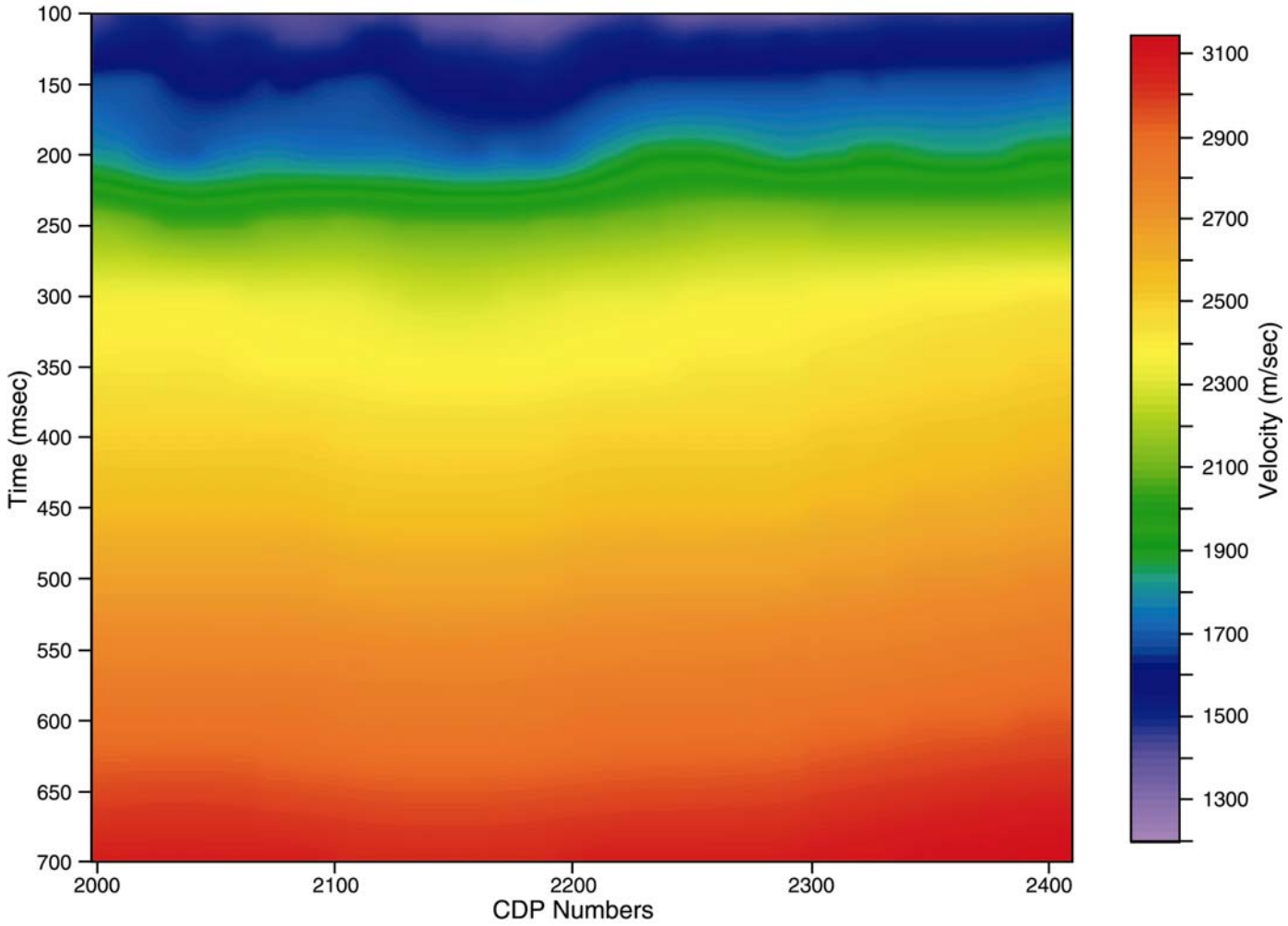

Figure 16: 2005 west-east velocity model used in the NMO correction during the processing flow.

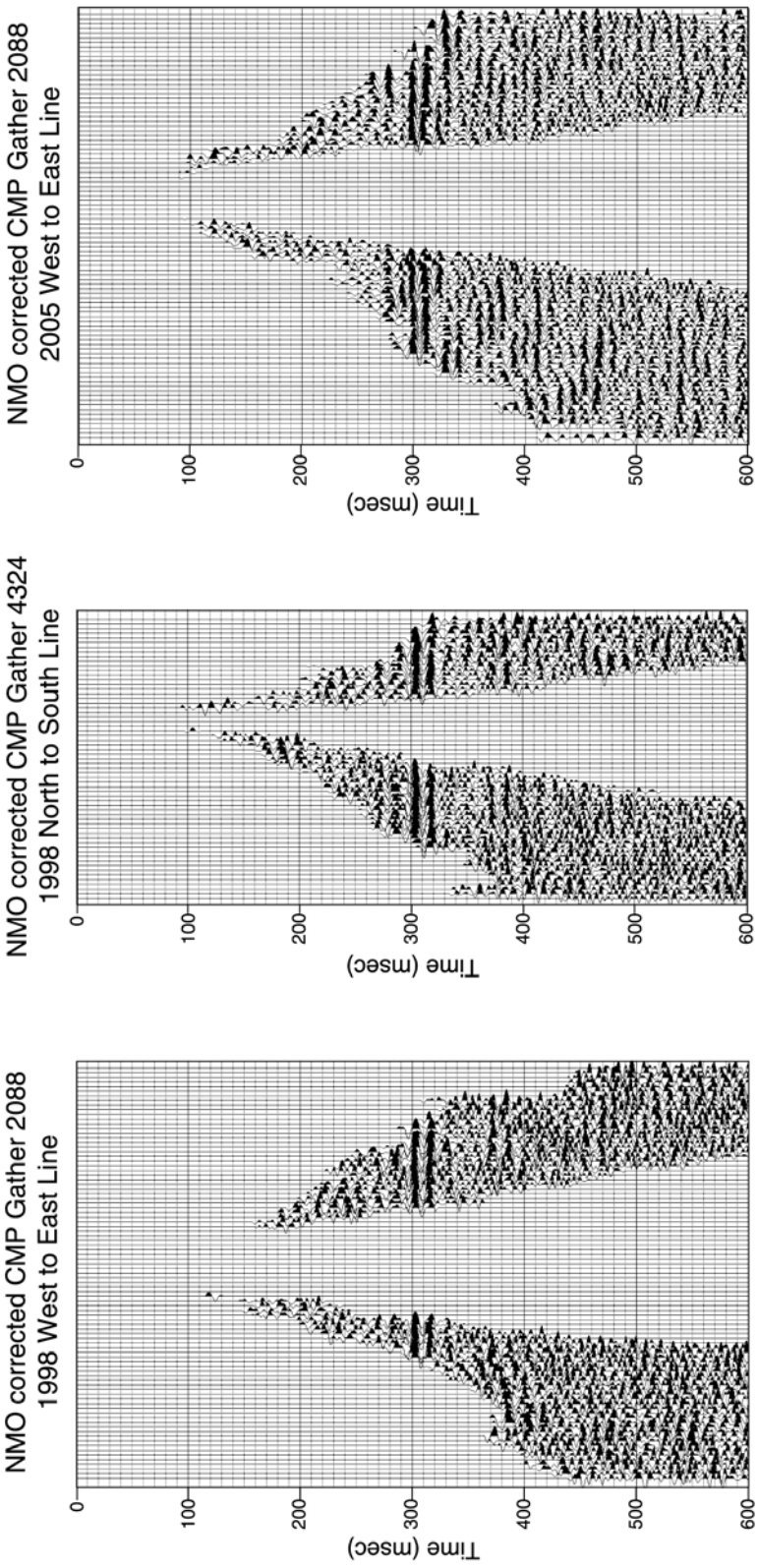

Figure 17: NMO corrected CMP gathers with muting and trace editing already applied.

beneficial in removing noise from the data (Ivanov et al., 1998). Maximum possible fold for CMP stacked sections was 102 nominal. After muting operations the CMP stacked sections (Figures 18, 19, and 20) had a maximum true fold of 80 nominal in the time window of interest (250 ms to 500 ms) (Figures 21, 22, and 23).

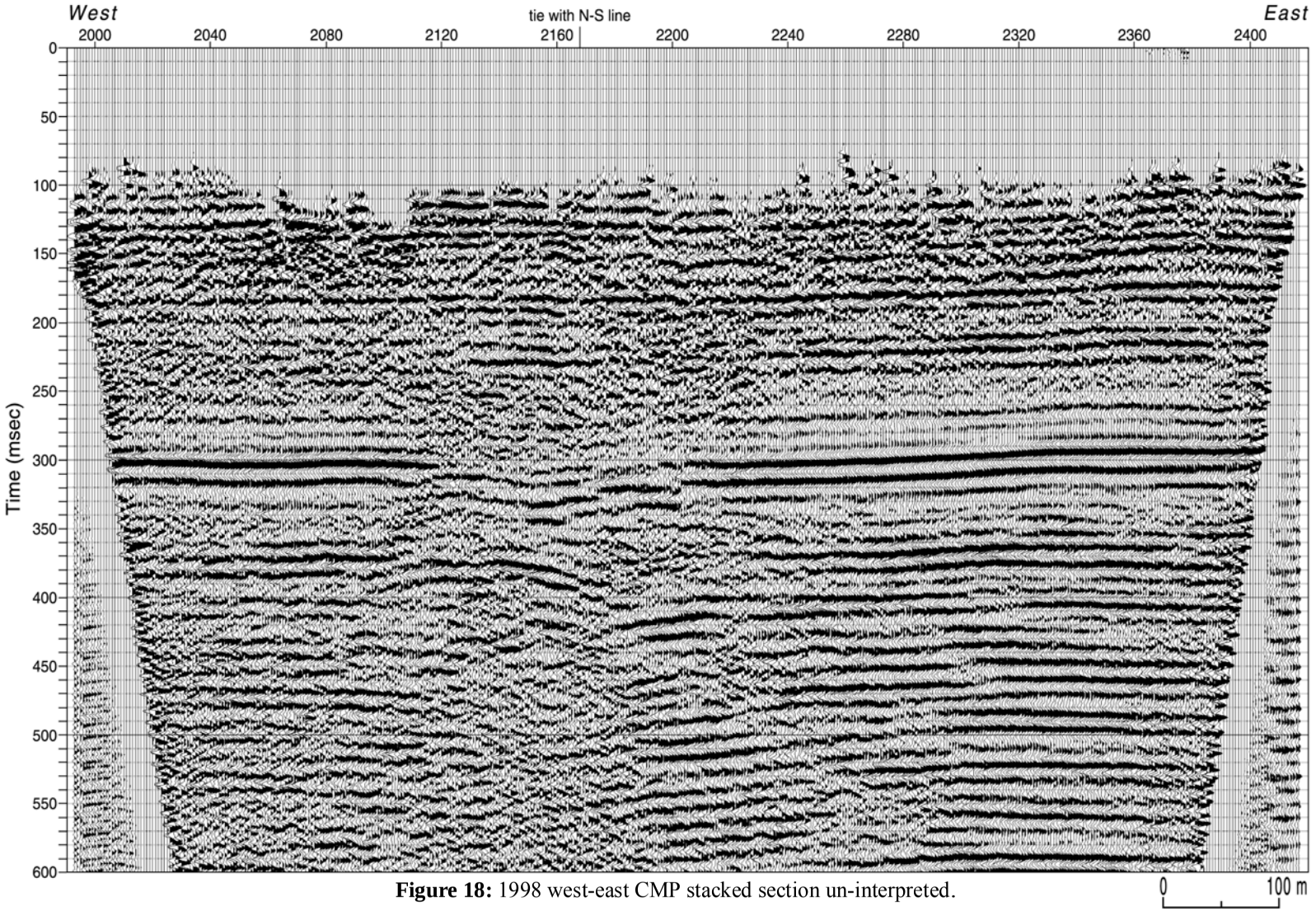

Figure 18: 1998 west-east CMP stacked section un-interpreted.

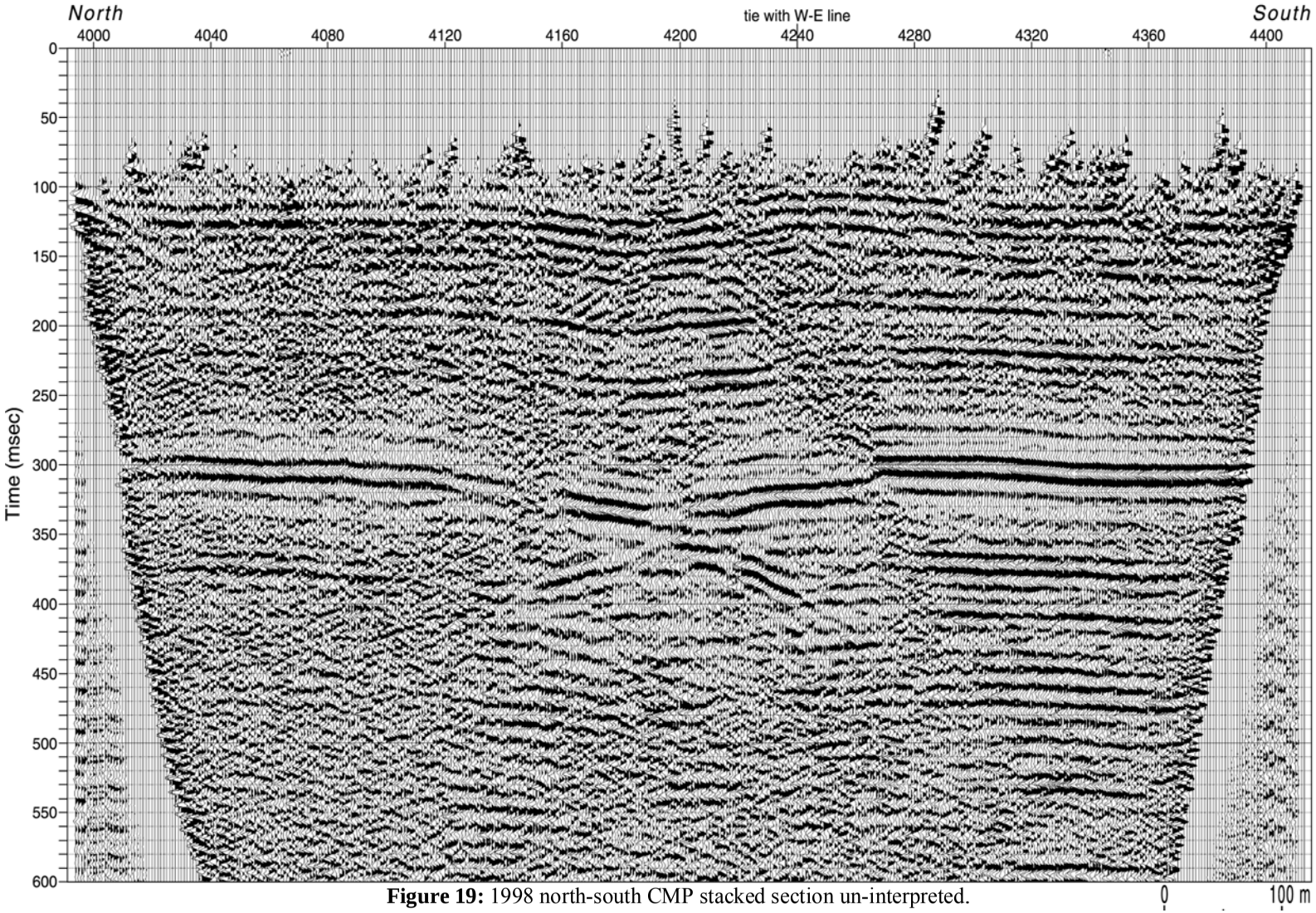

Figure 19: 1998 north-south CMP stacked section un-interpreted.

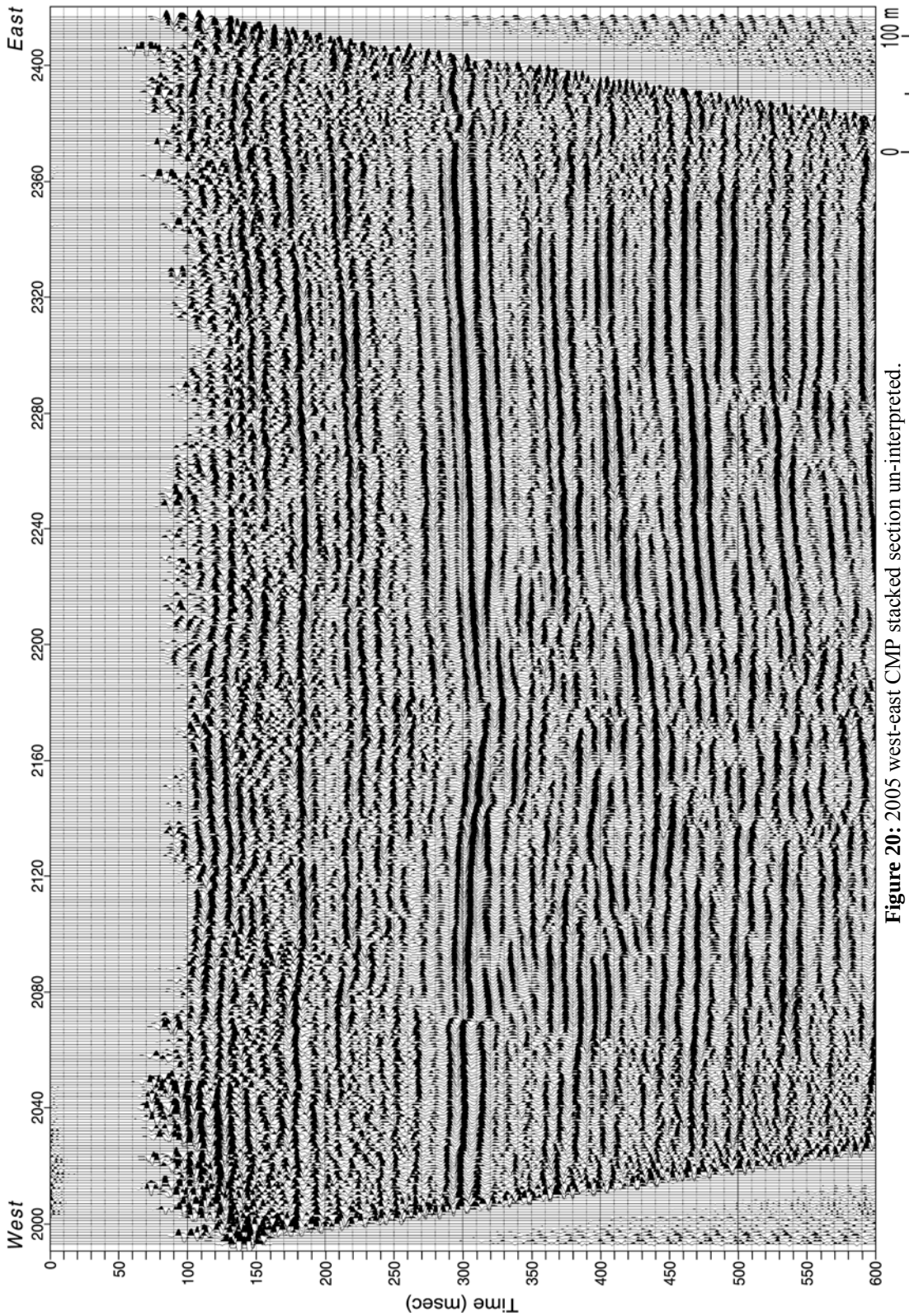

Figure 20: 2005 west-east CMP stacked section un-interpreted.

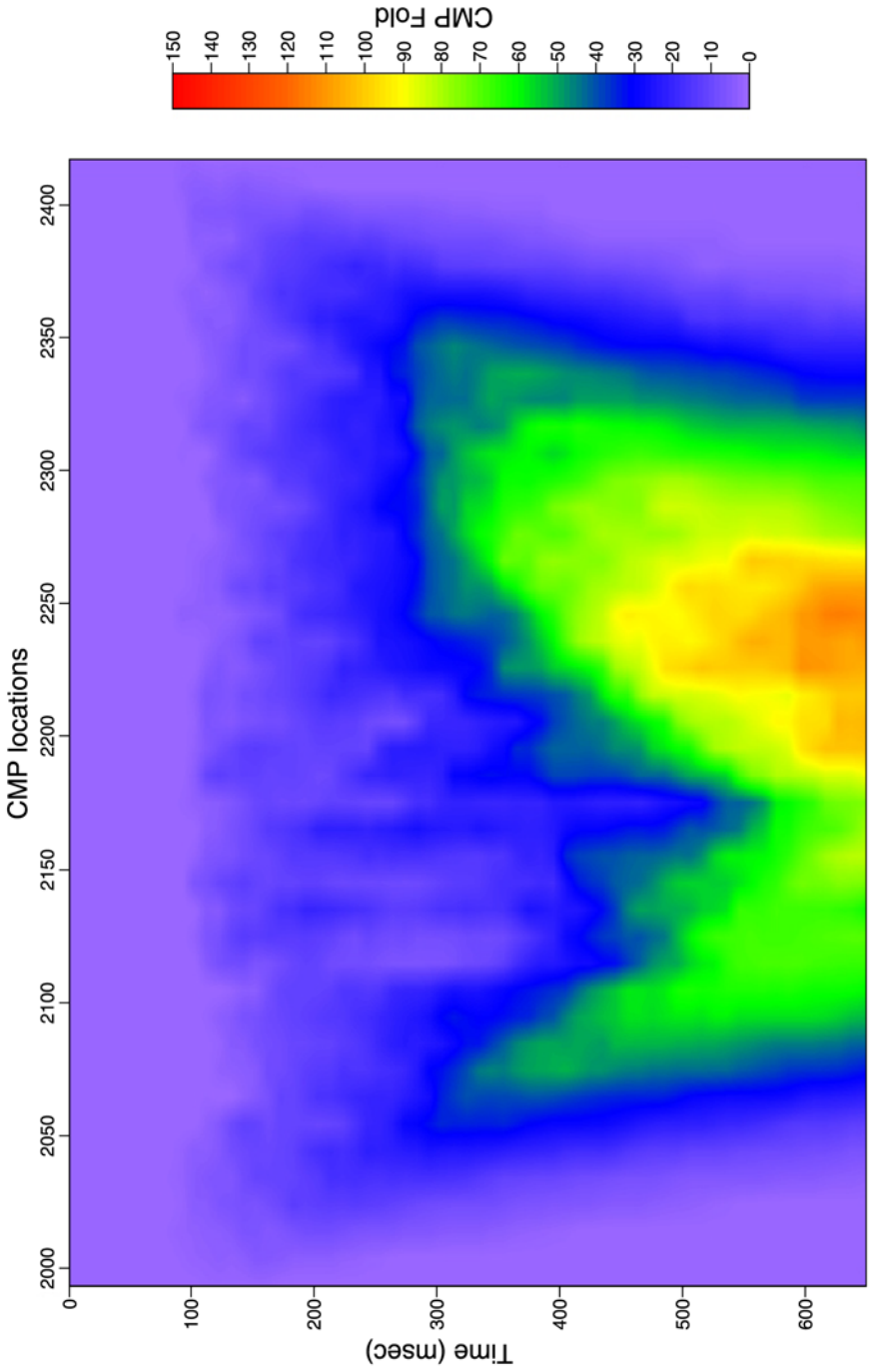

Figure 21: True fold map of CMP stacked section for 1998 west-east line.

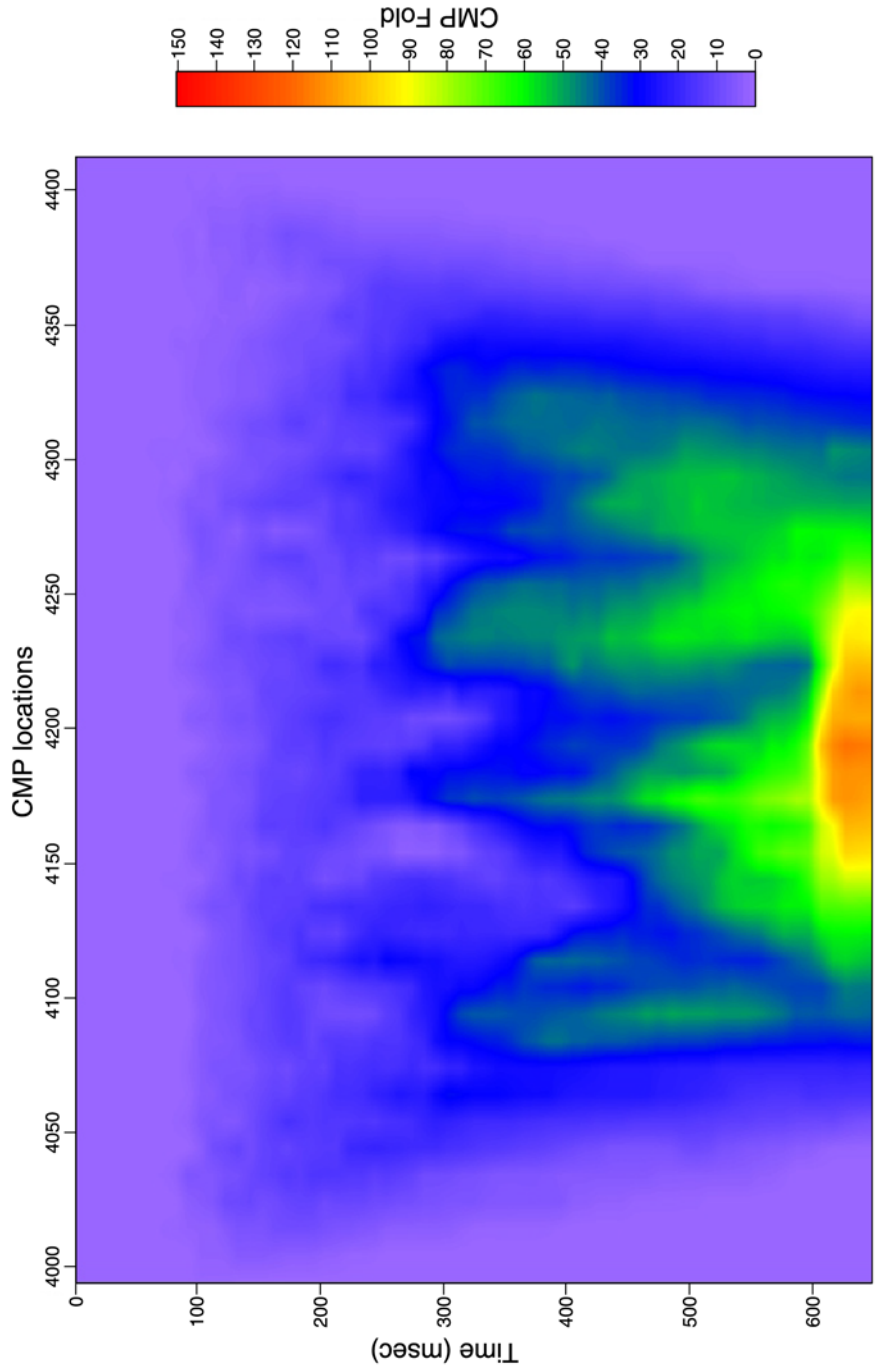

Figure 22: True fold map of CMP stacked section for 1998 north-south line.

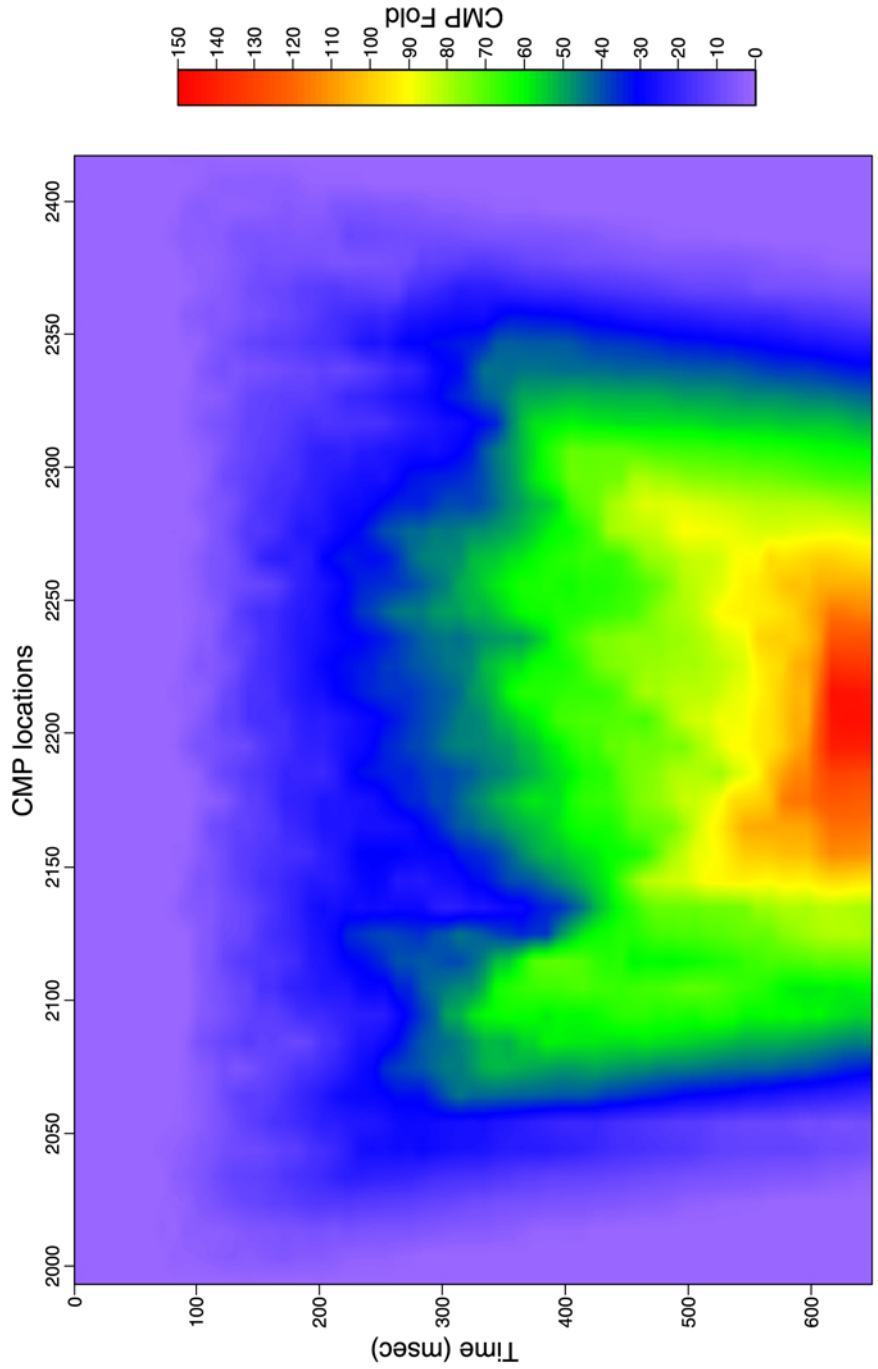

Figure 23: True fold map of CMP stacked section for 2005 west-east line.

Synthetic Seismogram

Borehole and electronic logs run in the Martin 1-36 well (T23S R16W, Sec. 36, E2 SE NE 3300 North, 330 West, from SE corner) approximately 2 km (Figure 24) from the Macksville sinkhole were used in the creation of a synthetic seismogram; effective in correlating reflections to reflectors. In 1995 electric logs were run in Martin 1-36 that included a gamma ray log that started approximately 73 m below ground surface (BGS) and ended 1250 m BGS. The sonic log data began at approximately 112 m BGS and concluded around 1250 m BGS. The full suite also included a porosity log.

The synthetic seismogram (Figure 25) was created using Kingdom Suite software. A 100 Hz Ricker wavelet was used to convolve with the reflectivity series generated from the sonic log. Since no velocity check-shot was collected in this well, the synthetic was time-tied to the CMP stacked sections. Therefore the synthetic seismogram was linearly stretched and squeezed between the reflections of the Stone Corral Formation and the top of the Chase group to match the seismic CMP stacked sections.

The program used to produce the synthetic did not compensate for attenuation nor did it include multiples in the idealized trace. These simplifications were not a problem since the synthetic was only used to correlate borehole depth to wavelet travel-time on vertically incident seismic data. This simplified synthetic actually helped distinguish primary reflections from multiples and therefore improved the geologic interpretations.

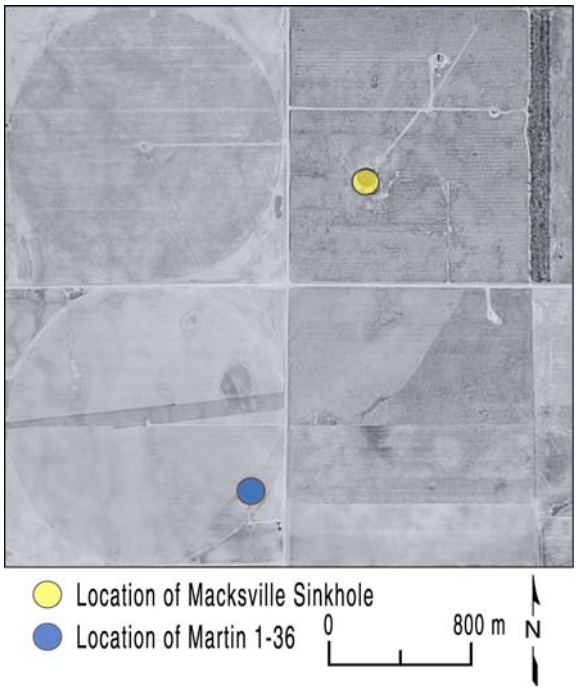

Figure 24: Location of Martin 1-36 well with sonic log in relation to the Macksville sinkhole (T23S R16W, Sec. 36, E2 SE NE 3300 North, 330 West, from SE corner).

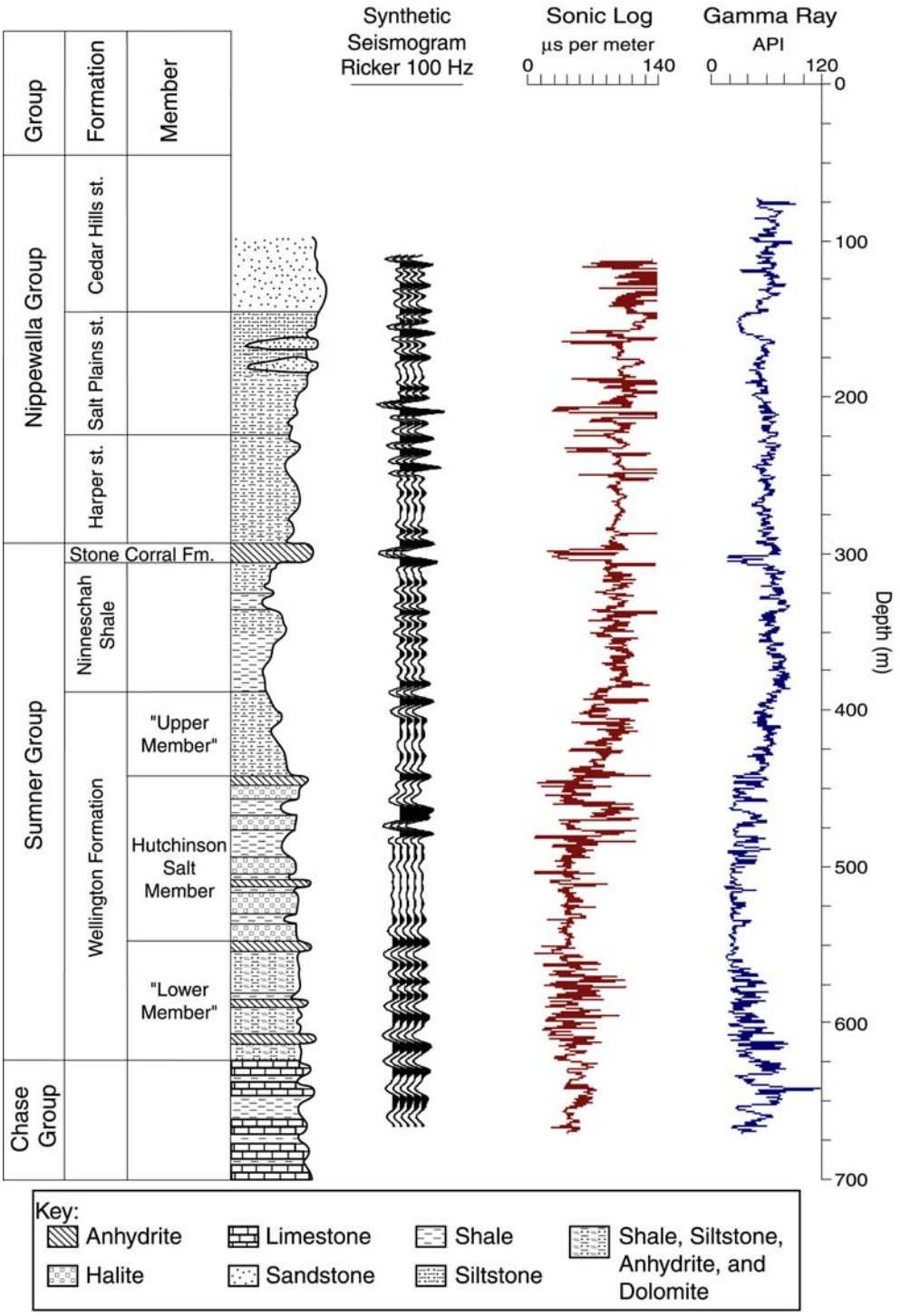

Figure 25: Synthetic seismogram from the Martin 1-36 well API 15-145-21425.

The synthetic seismogram, with key reflections marked, was correlated at a location on a CMP stacked section possessing the least bed deformation of the three CMP stacked sections (Figure 26, 27, and 28). The synthetic seismogram was then linearly stretched and squeezed until the high-amplitude synthetic seismic reflections matched up with their counterpart reflections on the CMP stacked sections (Figure 26, 27 and 28). These key high-amplitude reflections were then correlated across the entire stacked section. Slumping and failure above the dissolution-affected portions of the Hutchinson Salt Member can be easily interpreted from the changes observed in these major reflecting events.

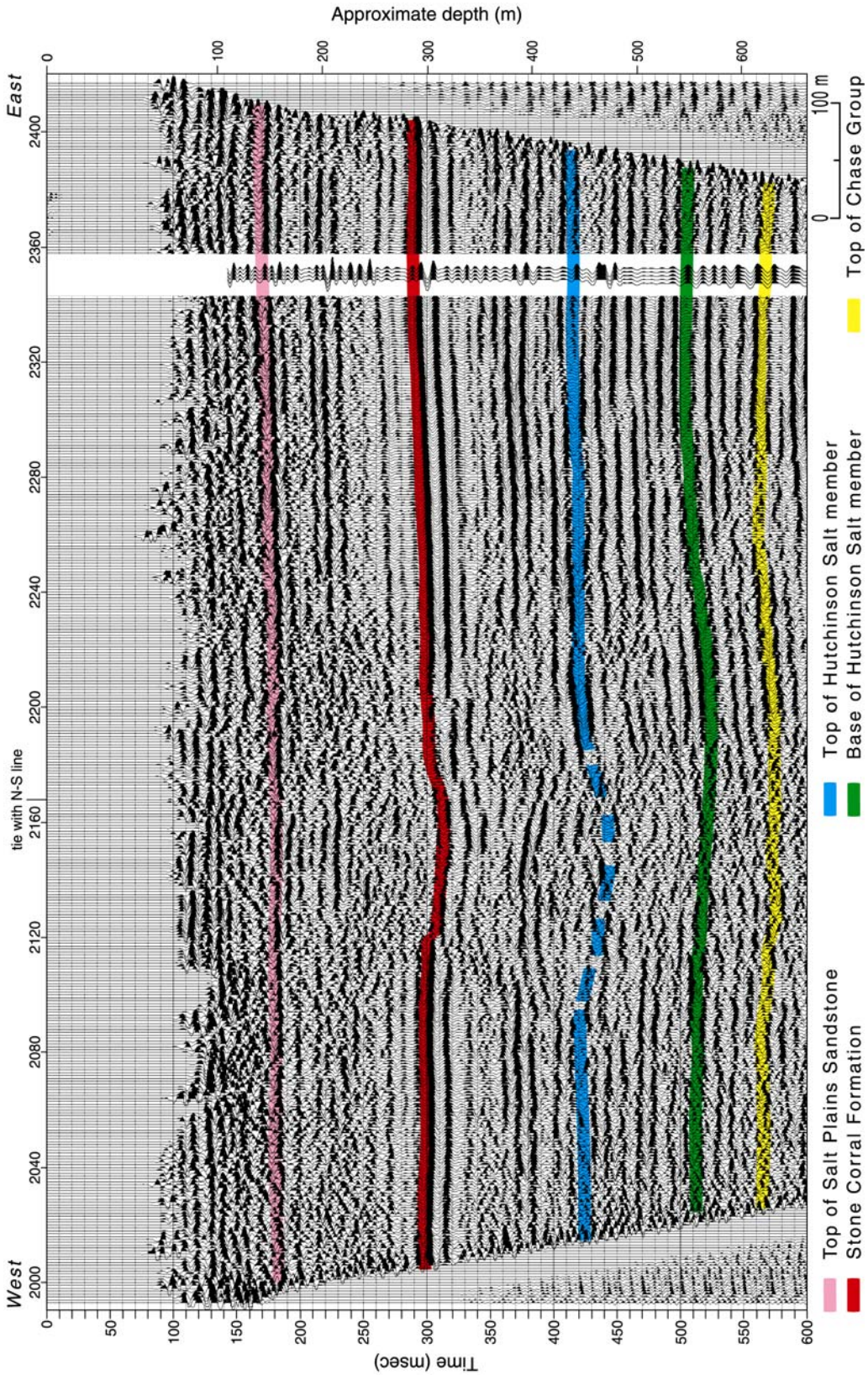

Figure 26: 1998 west-east CMP stacked section with tops information from the synthetic seismogram.

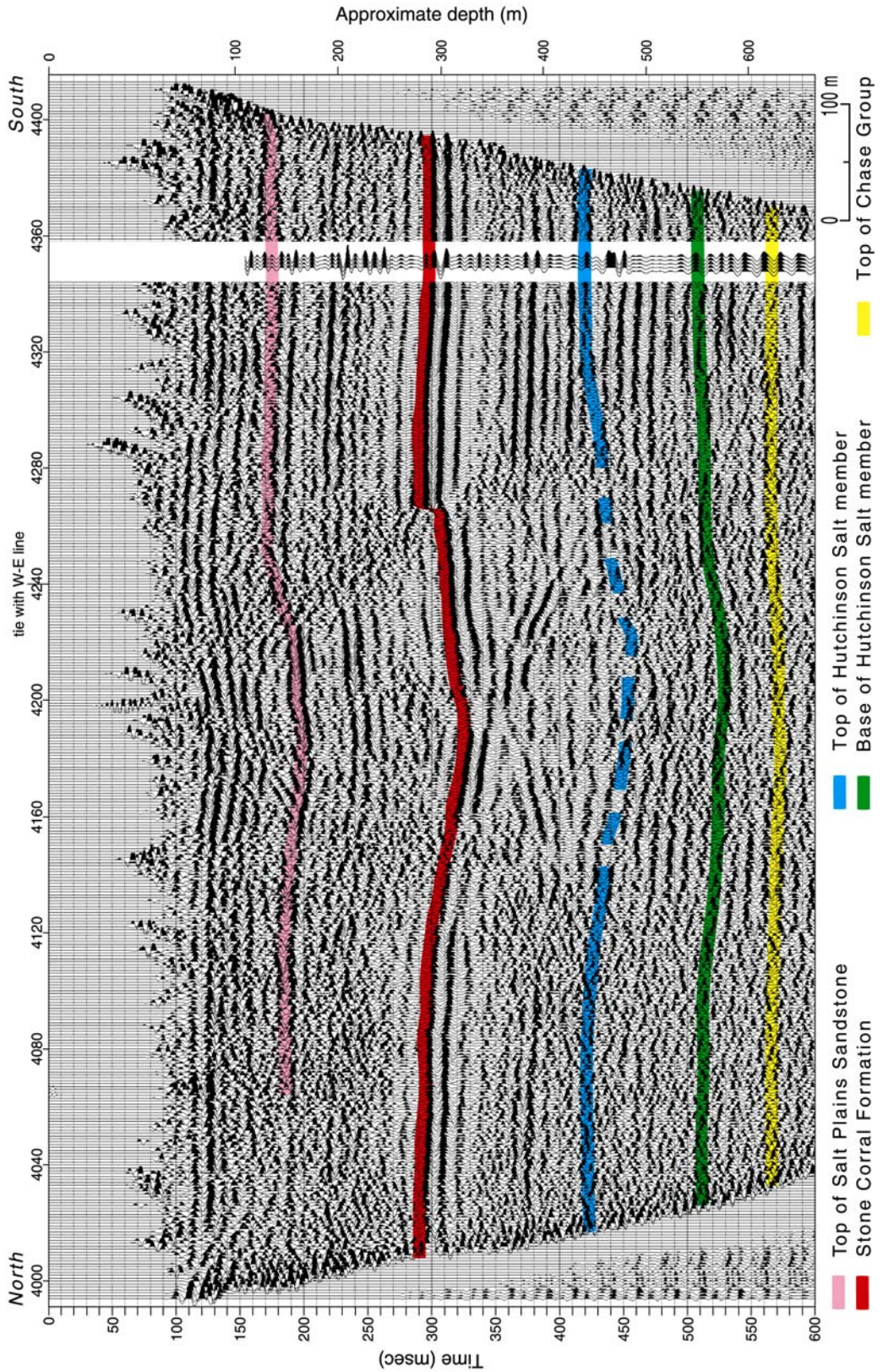

Figure 27: 1998 north-south CMP stacked section with tops information from the synthetic seismogram.

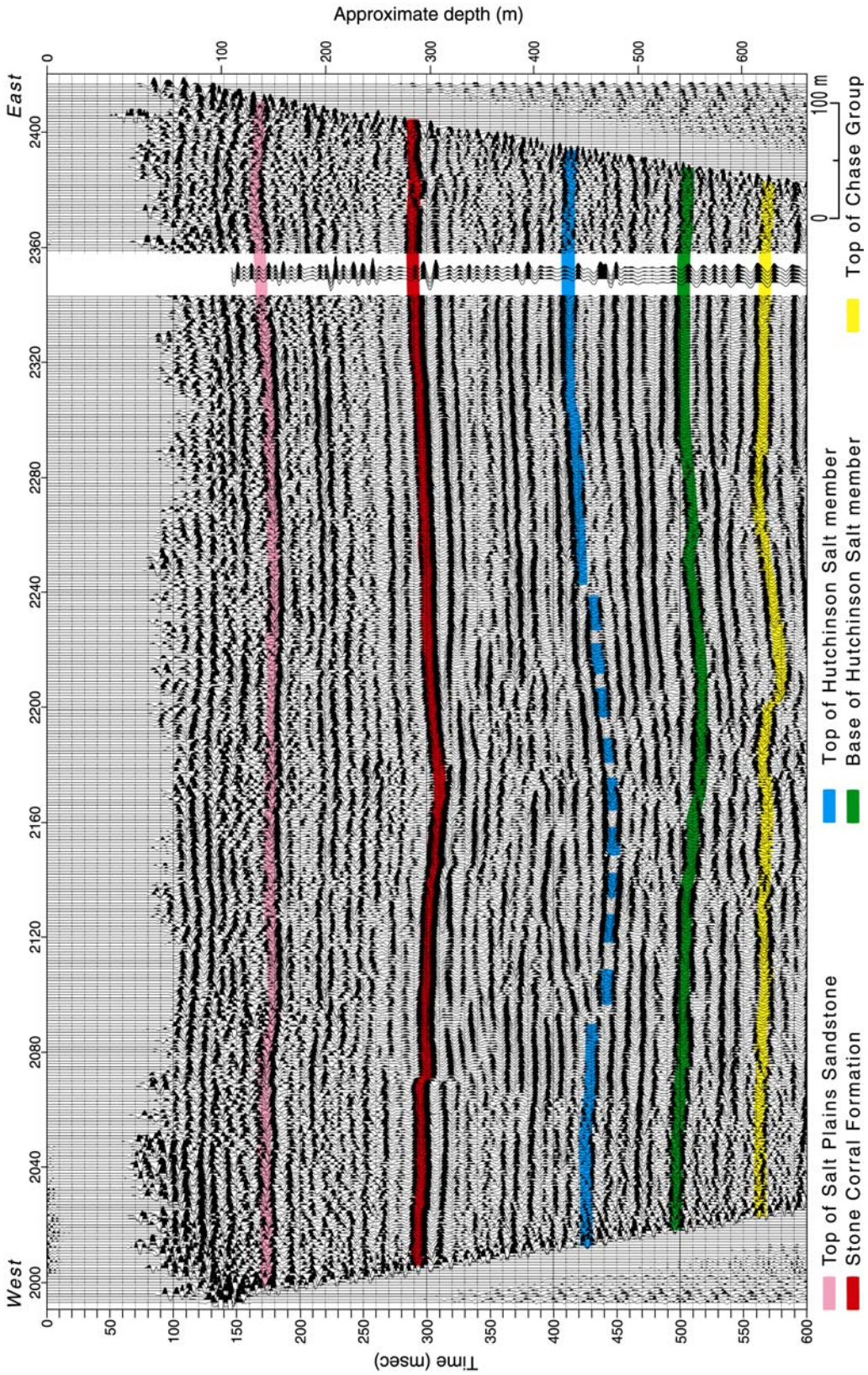

Figure 28: 2005 west-east CMP stacked section with tops information from the synthetic seismogram.

Results

Seismic Interpretation of the Macksville Sinkhole Data

Confident identification of reflections on shot gathers is essential to accurate processing and interpretation of shallow seismic-reflection data. Identifying interpretable reflections on shot gathers is crucial in differentiating reflections from stacked coherent noise events present in the early-time part of the shot gathers. If reflections are not properly interpreted and tracked throughout the processing flow, artifacts are not only possible but probable. Reflections recorded during both from the 1998 and 2005 surveys are easily interpreted and can be correlated to geologic contacts identified on Martin 1-36 well logs on both shot gathers and CMP stacked sections (Figures 26, 27, and 28).

Coherency is sufficient to interpret reflections across most traces on shot gathers throughout the primary time-depth target window (250 ms to 600 ms). Individual reflection events cannot be traced through the air-coupled wave and ground-roll wedge on shot gathers. Asymmetry of reflection hyperbolae observed on shot gathers from all lines is the result of dipping layers and lateral velocity variability in the immediate vicinity of the sinkhole. These distortions adversely affected the effectiveness of standard NMO velocity corrections.

Vertical bed resolution within the Hutchinson Salt Member is approximately 18 m (assuming ¼ λ, Widess, 1973). This was ample resolution potential for confidently interpreting rock layers distorted after collapse into voids left in the rock-salt from leaching. The reflection from the Stone Corral anhydrite varies in depth

across the profiles but generally arrives around 300 ms two-way travel time, corresponding to an approximate depth of 290 m. The reflection from the top of the Hutchison Salt Member arrived between 420 ms and 515 ms two-way travel time depending on the CMP location relative to the sinkhole. These two-way travel times corresponds to depths of approximately 440 m to 550 m (Figures 26, 27, and 28).

Initial failure resulted in catastrophic formation of the sinkhole's first surface expression. The failure occurred along high-gradient lines of stress as defined by the tensional dome (Figure 29). This failure mechanism resulted in an upward-narrowing chimney feature confined by the fault features defining the highest stress lines and weakest rock properties of the tensional dome. Changes in the dip angle and location of disturbed layers through this chaotic zone provide evidence that helps decipher the sequence and timing of subsidence that has led to the current sinkhole.

The 1998 north-south CMP stacked section shows signs of two separate instances of tensional dome failure (Figure 30). The innermost reverse faulting (shown in blue) defining this upward-narrowing chimney and defining the extent of the roof-rock collapse appears to have truncated before reaching the ground surface. Therefore, the initial collapse never reached the ground surface and was therefore not discovered. There was a second episode of roof-rock failure when the upward-narrowing chimney feature reached the surface forming a sinkhole. This second failure was likely the event responsible for the catastrophic surface collapse in 1988. With these data sets it is impossible to determine when the initial failure occurred. It is unknown at this time if this first failure occurred years, months, days, or nearly

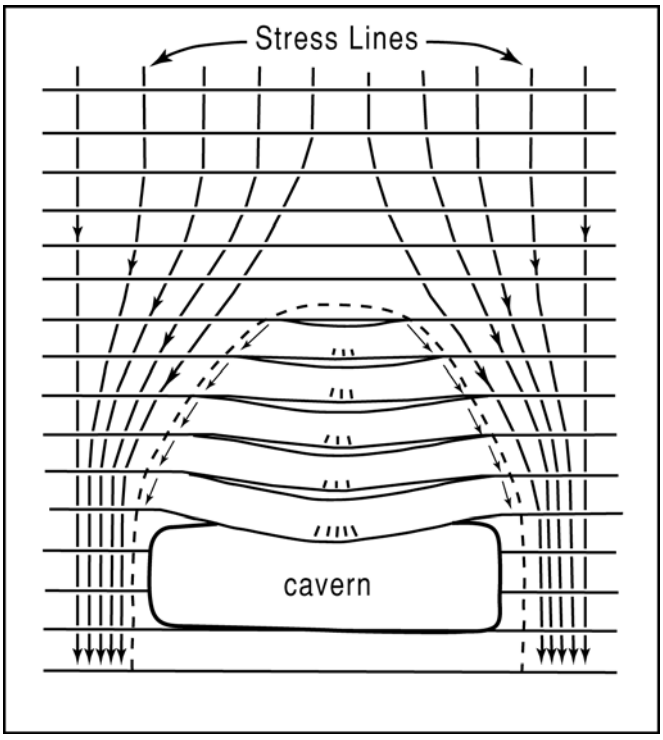

Figure 29: Depiction of the tensional dome and distribution of stress around a cavern opening in horizontal strata
(Davies, 1951).

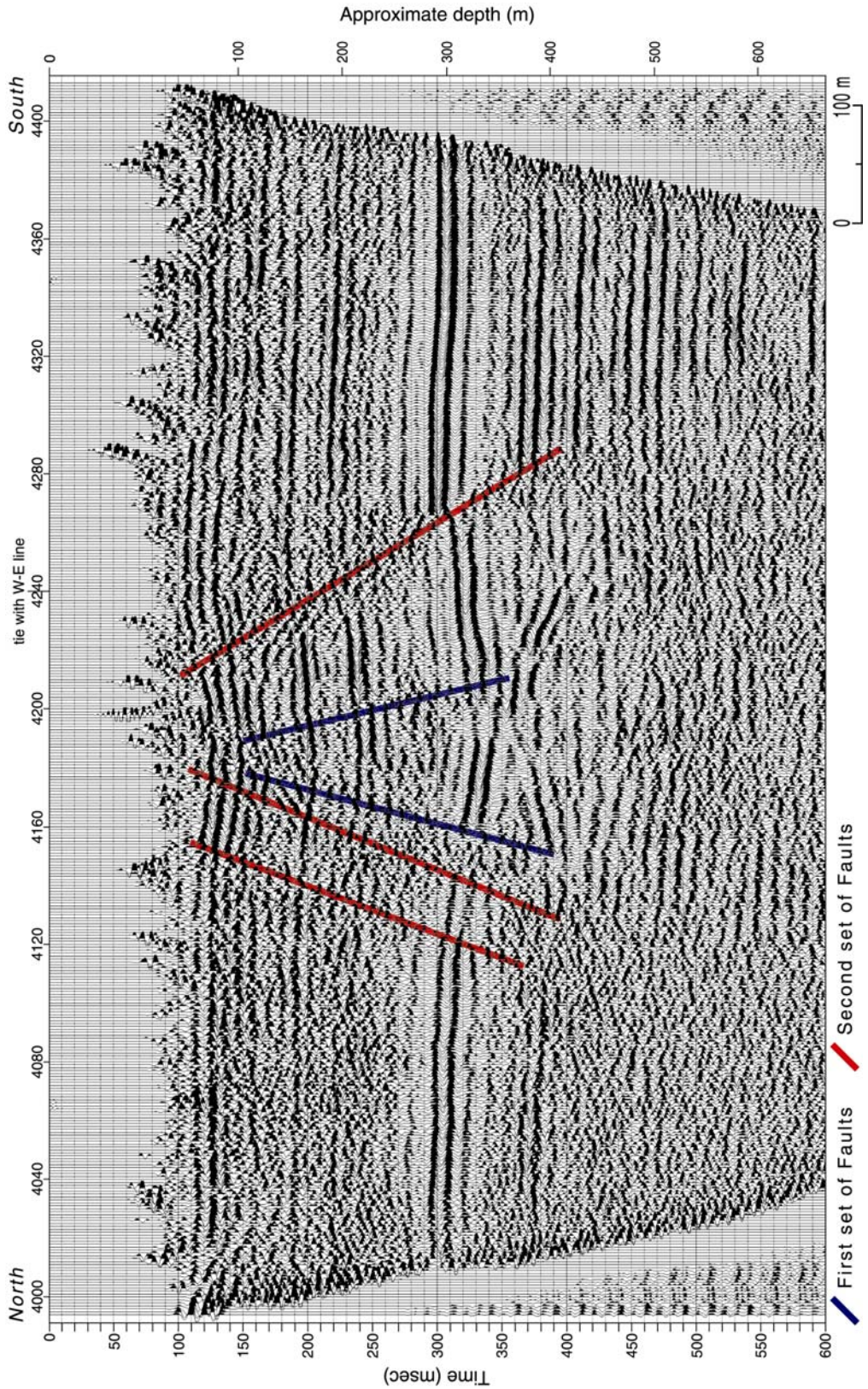

Figure 30: 1998 north-south interpreted CMP stacked section.

coincident with the second failure.

Time-Lapse Interpretation

Significant change in the signal-to-noise ratio is evident between the two west-east lines from 1998 (Figure 18) and 2005 (Figure 19). The signal-to-noise ratio (S/N) for the 2005 west-east survey improved in comparison to the 1998 west-east survey. The signal-to-noise ratio of the 2005 west-east data is also greater than the 1998 north-south survey. Improved energy transmission and response of both source and receivers and in signal amplitudes during 1998 is likely key to the observed decrease in signal-to-noise ratio relative to 2005. Changes in coupling and/or surface or very near-surface soil-moisture conditions are key to these kinds of differences**.**

Slumping of the reflections above the salt is evidence of subsidence (Knapp et al., 1989) and suggests dissolution. An examination of the difference in apparent slumping in the reflections between the two west-east surveys was conducted. The high-amplitude wavelet peaks interpreted in the 1998 west-east CMP stacked section (Figure 31) were overlain on the 2005 west-east CMP stacked section (Figure 32). This comparison was only possible after detailed processing that focused on amplitude equalization from one data set to the other. Interpretations were not conducted within the tensional dome due to uncorrectable velocity anomalies. Portions of the 2005 west-east CMP section were enlarged to study distortions in the rocks and bed geometries above and within the salt interval more closely (Figure 33 and 34). From regional geological maps, we know that rock layers were horizontal before initiation of salt dissolution. Slumping events within the Hutchinson Salt

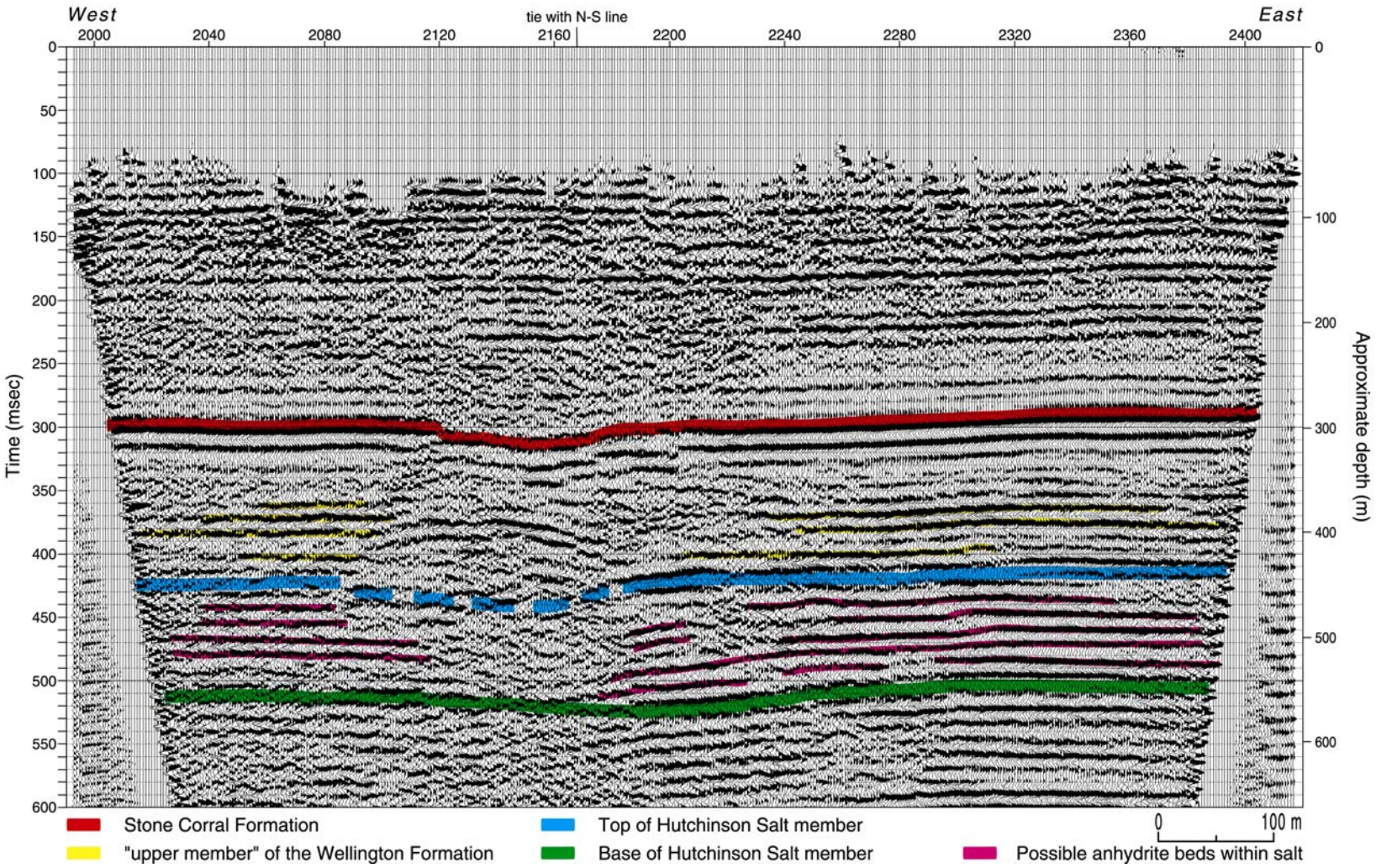

Figure 31: 1998 west-east CMP stacked section with reflection interpretations on wavelet peaks.

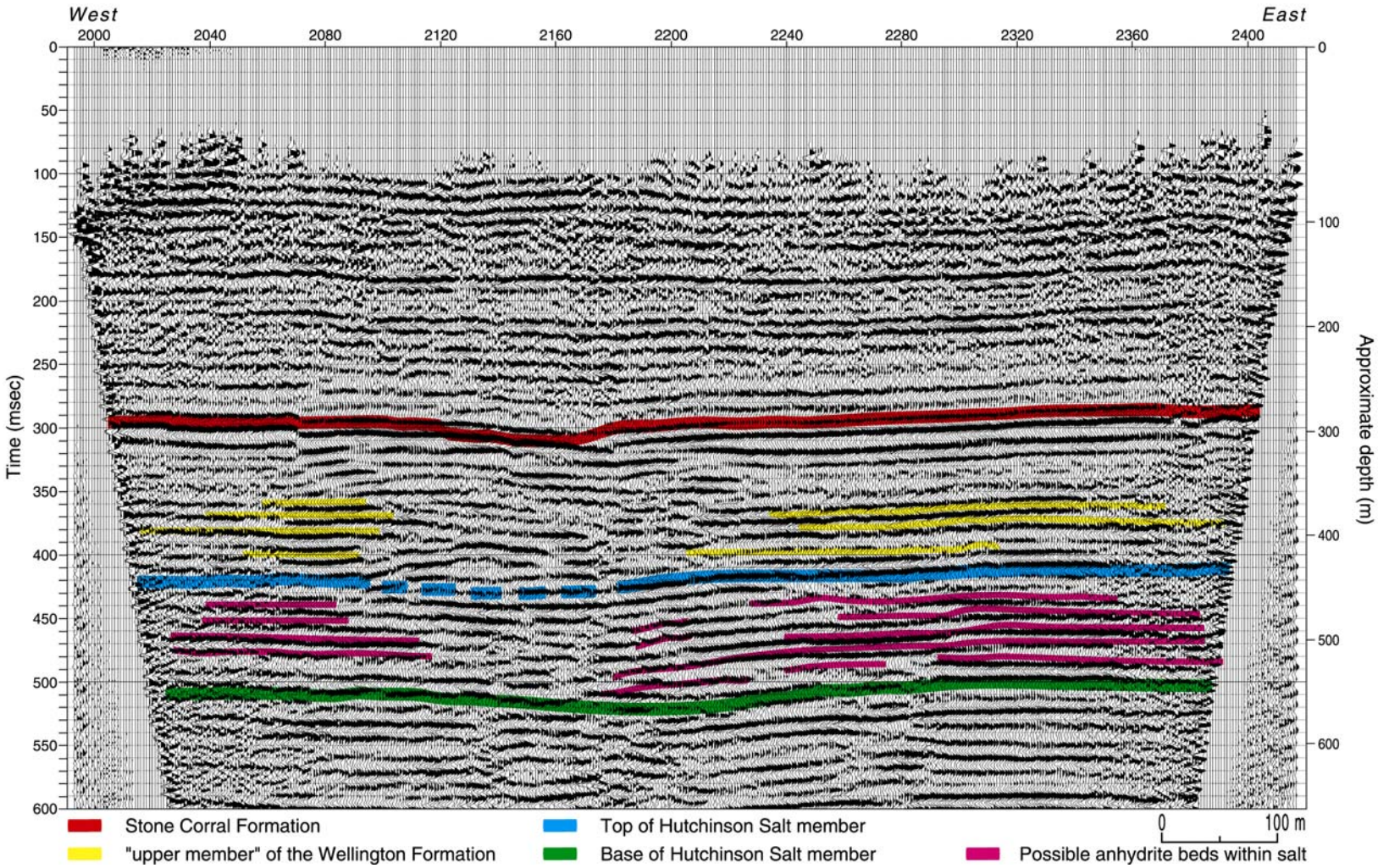

Figure 32: 2005 west-east CMP stacked section with 1998 west-east reflection interpretations on wavelet peaks overlain.

Member (Figure 33 and 34) extrapolated vertically to the Stone Corral Formation is evidence of ductile failure. Beds above the Stone Corral Formation do not appear distorted to the degree observed in rocks directly over the salt. Bed distortion is more evident east (Figure 34) of the old disposal well relative to west of it (Figure 33).

Dissolution areas at the time of the 1998 survey were interpreted based on slumping beds and extended more than 240 m north, 245 m south, 400 m east, and 200 m west of the approximate original disposal well location. This area of distortion interpreted on the 1998 sections (Figure 31) overlain on the 2005 data (Figure 32) had advanced to the east approximately 125 m and 100 m in the westerly direction. Changes in the salt dissolution and associated slumping of the overlying beds on the 1998 (Figure 35) and 2005 (Figure 36) west-east lines inferred from seismic data are consistent with the surface expressions. There is a preferential eastward dissolution in the salt interval that is evident in the surface expression and subsurface dissolution. The interbedded nature of the Hutchinson Salt Member could influence a channelized dissolution pattern with a very erratic progression through the salt leaving areas more resistant to dissolution behind the dissolution front. Without a 3-D seismic survey this cannot be clearly defined.

Documented Surface Subsidence

The KCC has collected data at a set of points around this sinkhole since its formation in 1988 (Figure 37). Changes in the surface expressions since the sinkhole's formation appear to be predominantly to the east with a markedly slower rate of change to the west (Figure 38). Since 1991 the change in elevation has been

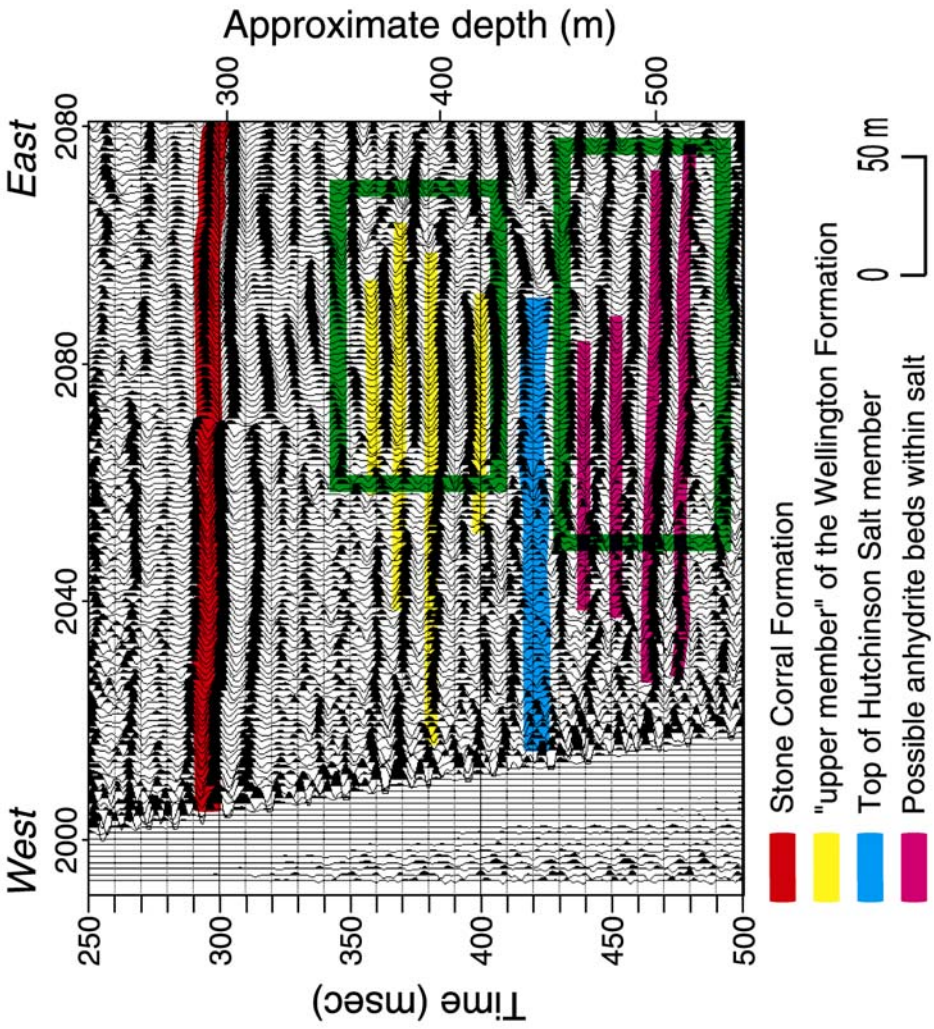

Figure 33: Detail section of the west side of figure 33 (2005 west-east CMP stacked section with 1998 west-east reflection interpretations on wavelet peaks overlain.). Green squares highlight areas of slumping since 1998.

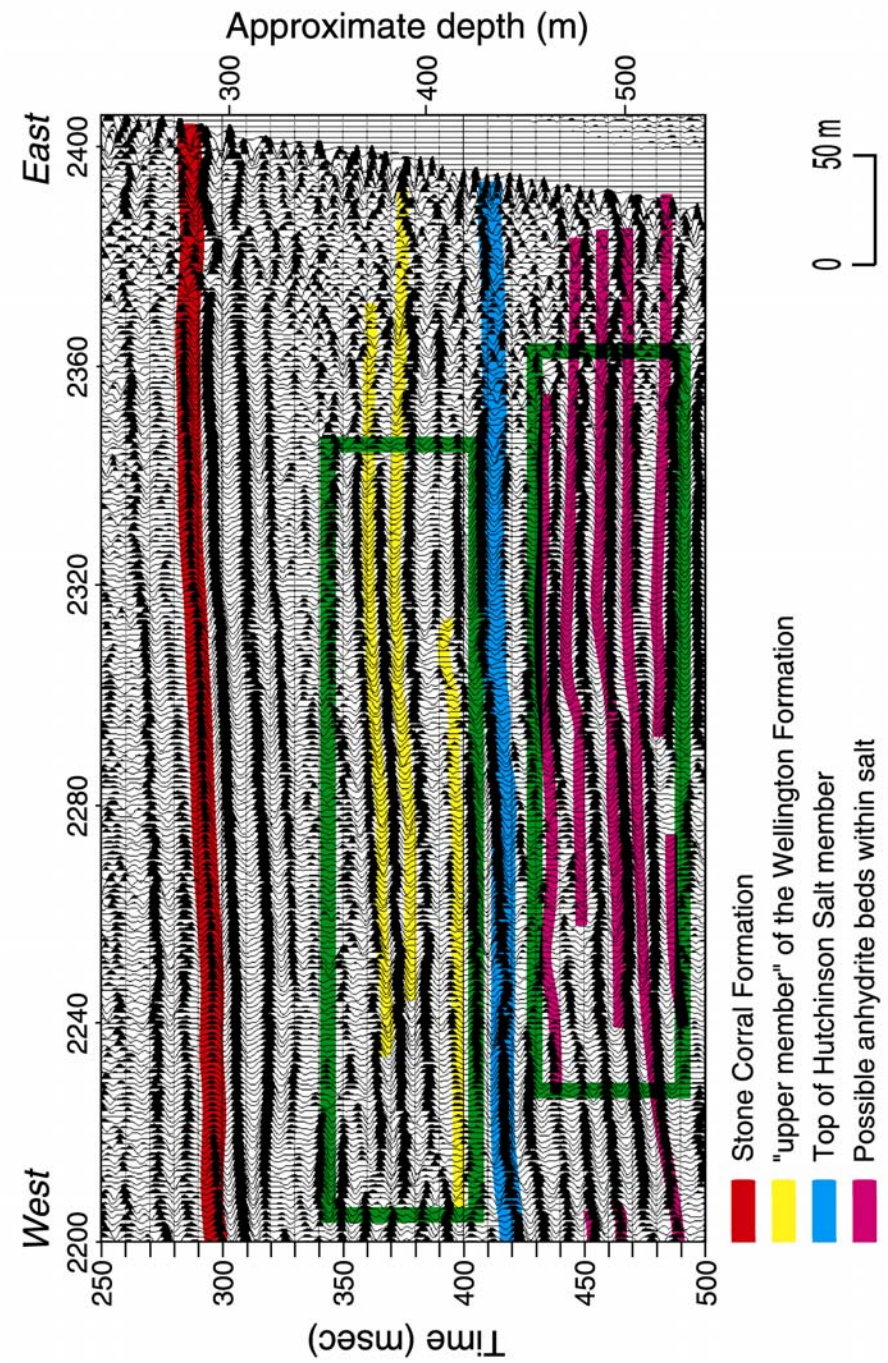

Figure 34: Detail section of the east side of figure 33 (2005 west-east CMP stacked section with 1998 west-east reflection interpretations on wavelet peaks overlain). Green squares highlight areas of slumping since 1998.

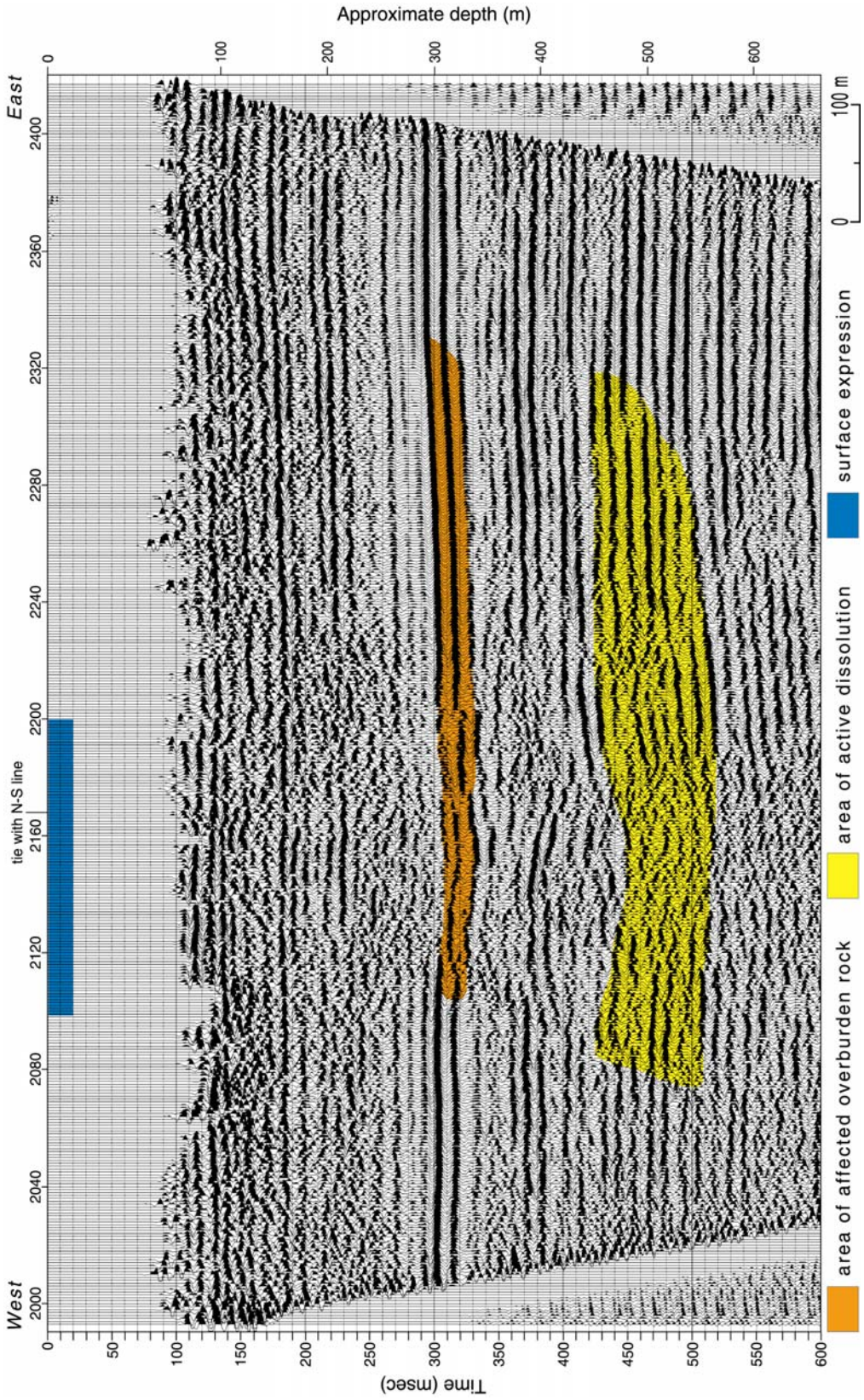

Figure 35: 1998 west-east interpreted CMP stacked section.

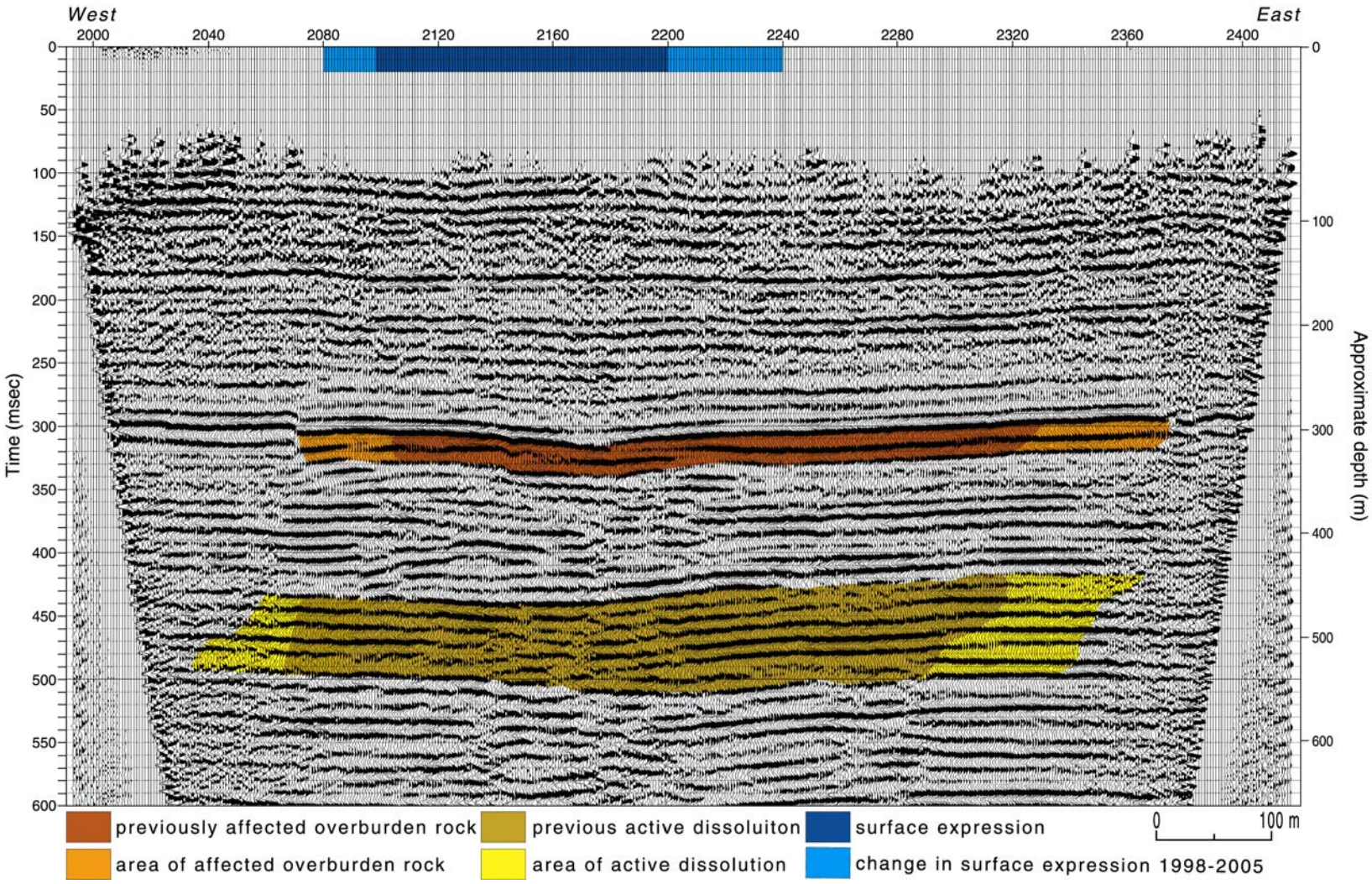

Figure 36: 2005 west-east interpreted CMP stacked section.

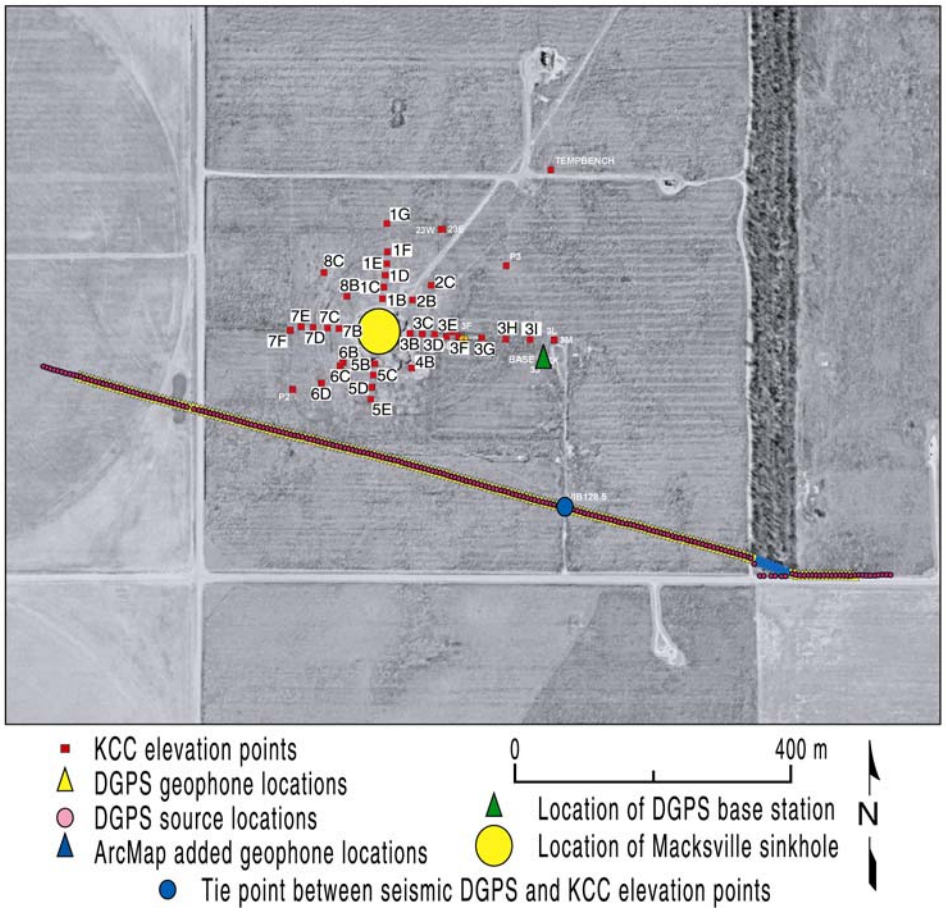

Figure 37: Orthophoto overlaid with the 2005 KCC elevation points collected in DGPS format and the DGPS seismic line.

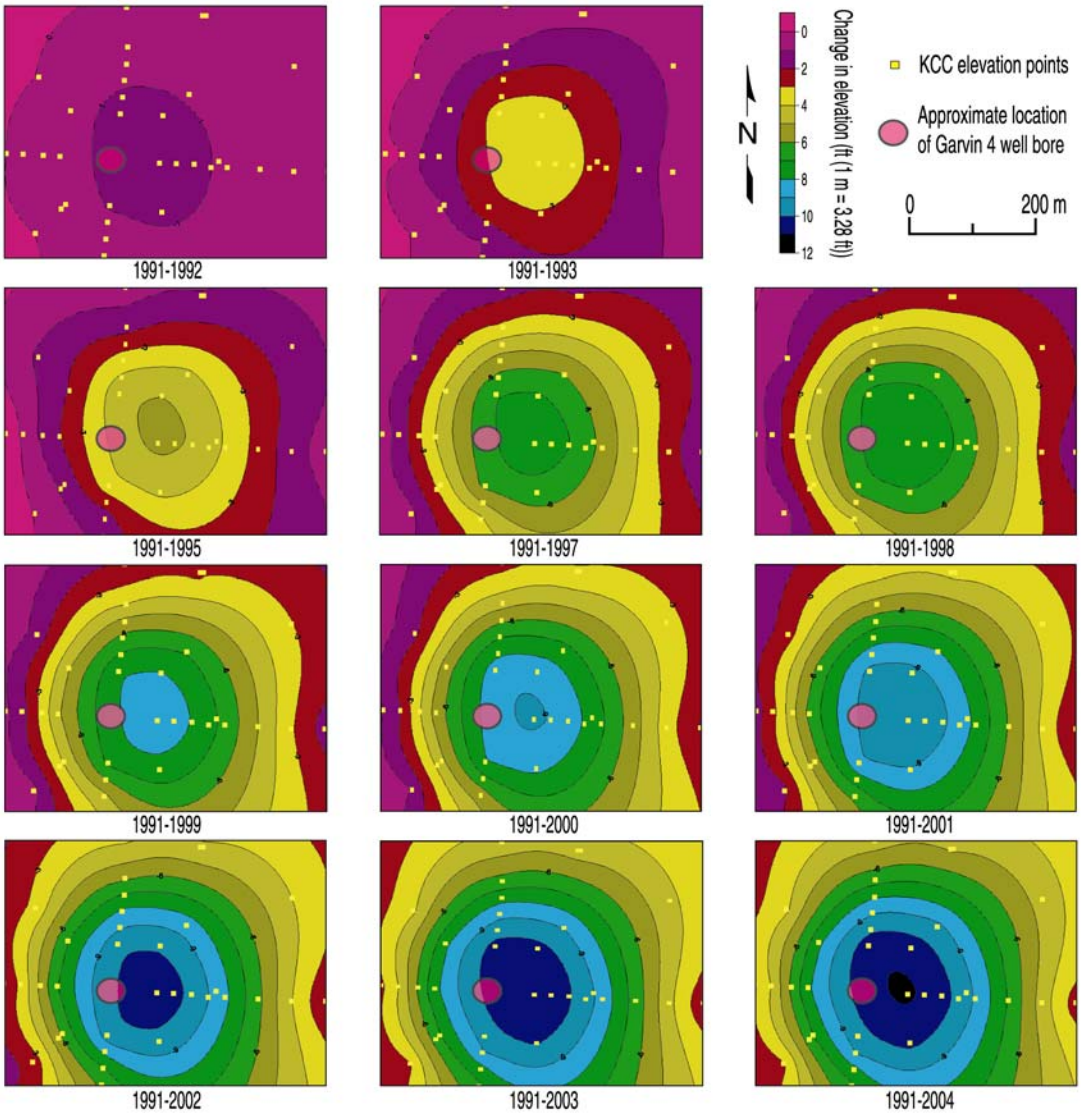

Figure 38: KCC elevation points depicting the relative change in surface expression over time.

significant to the north and east of the well with subsidence slowing from 2003 to 2004 relative to all previous years monitoring (Figure 39).

An analytical method was attempted to establish trends in the subsurface and surface data. Three data points were approximated using the seismic data to find the subsurface horizontally affected area: initial collapse; extent of dissolution in 1998; and affected dissolution extremes interpreted on 2005 images (Figure 40). These points approximately fit to ($y = a * Ln(x) - b$) curve. The KCC west and east surface data points (Figure 38) were used to find the change in elevation. This elevation data from KCC was used to find a surface (Figure 41) to subsurface (Figure 40) correlation in subsidence growth. The surface elevation data shows a possible plum elongated to the northeast, east, and southeast direction. The subsurface dissolution appears to be progressing to the northeast and southeast as well as to the east (Figure 36).

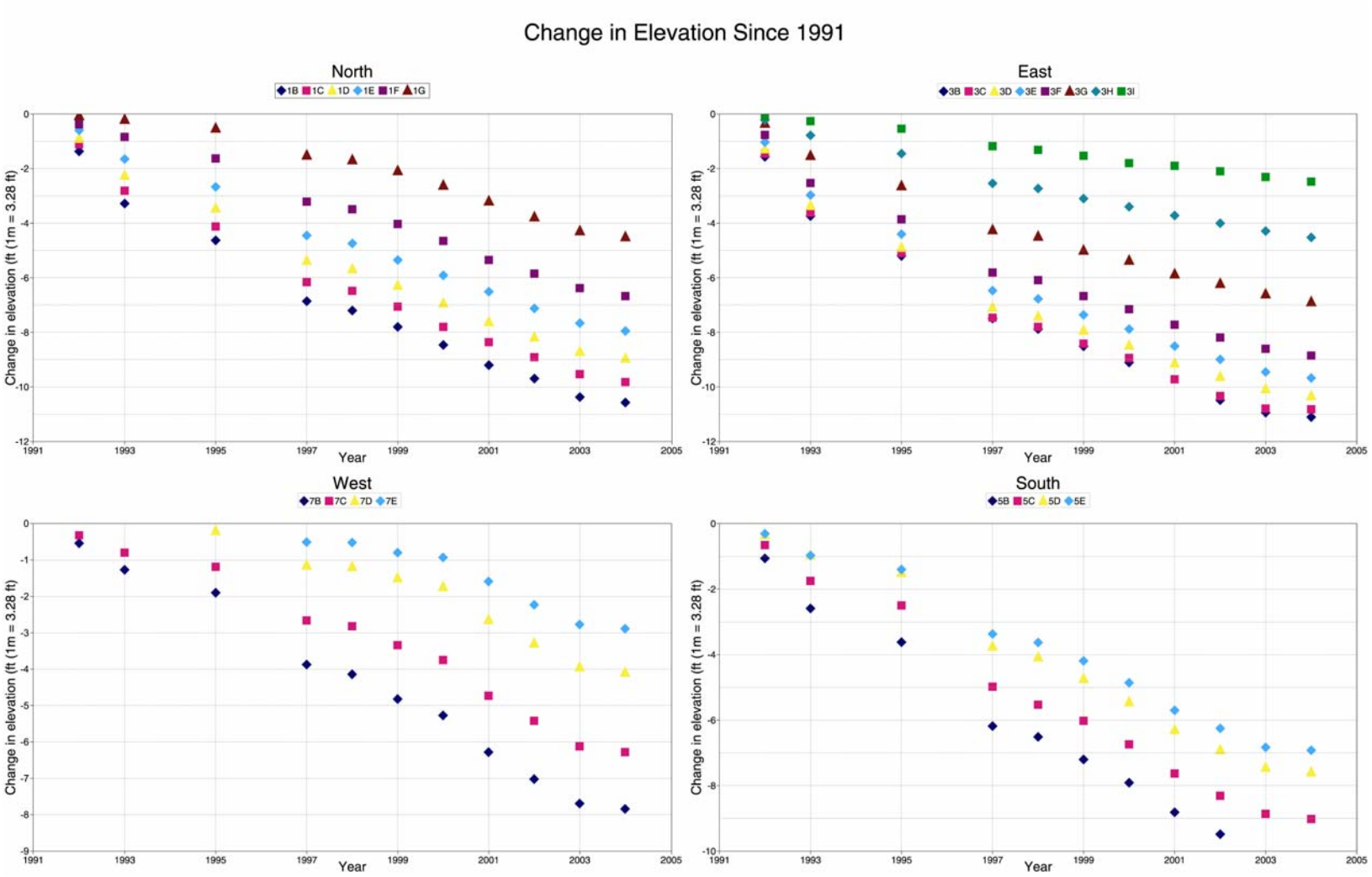

Figure 39: Directional change in elevation since 1991

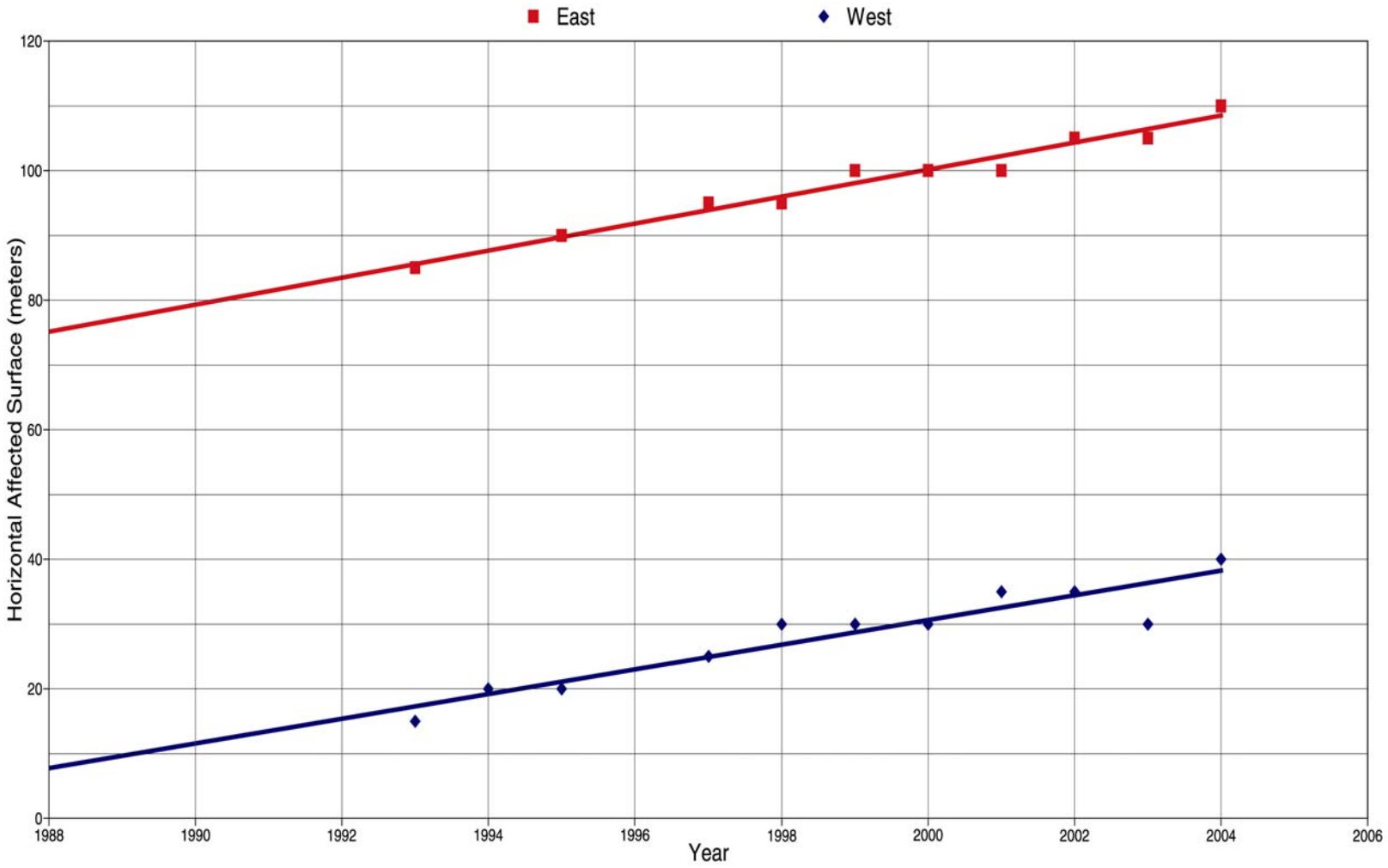

Figure 40: Graph of surface expression growth over time using the KCC elevations points.

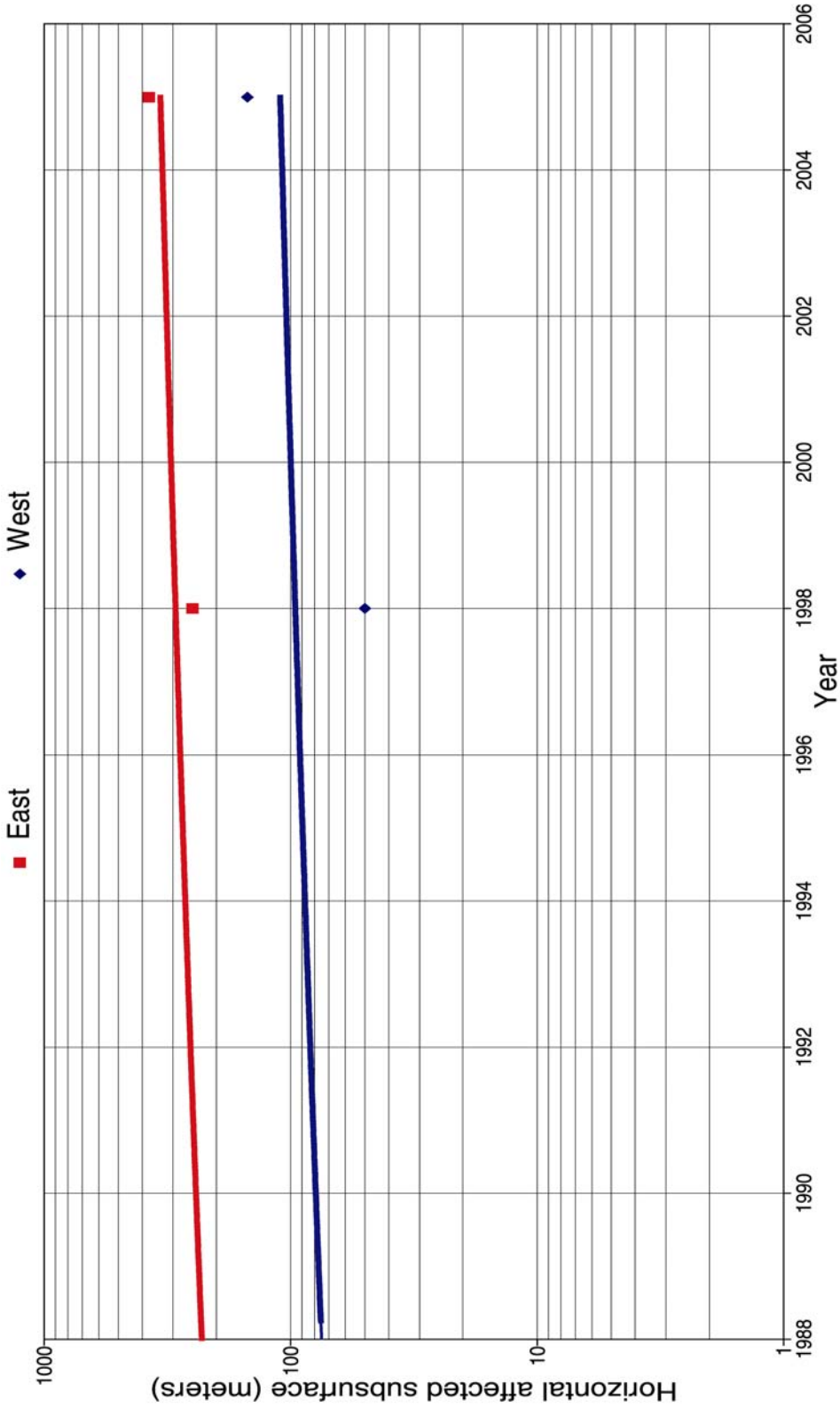

Figure 41: Graph of subsurface dissolution over time.

Discussion

Sinkholes seismically investigated around disposal wells generally appear roughly symmetrical in the subsurface about the culprit well bore (Miller et al., 1988; Knapp et al., 1989; Miller et al., 1990; Miller et al., 1995; Miller et al., 1997; Miller et al., 2002). This uniform dissolution pattern does not appear to be the case for the Macksville sinkhole. Both surface and subsurface expressions are clearly elongated to the east (Figure 40 and 41).

While the initial appearance of the Macksville sinkhole took a matter of only hours. Other sinkholes associated with disposal well failures in nearby Stafford County investigated with high-resolution seismic reflection formed gradually and symmetrically. The St. John Northwest Oil and Gas Field is home to the French sinkhole (formed in 1991) while the Leesburg sinkhole formed in 1992 in the Leesburg Oil and Gas Field. Mapping the edge of the affected surface of these sinkholes in aerial photos taken in 2002 allows some comparison of the surface dimensions to the Macksville sinkhole (Figure 42).

The Macksville sinkhole formed before the French and the Leesburg sinkholes. The Macksville sinkhole's surface area in 2002 was not as large as the other's. This suggests subsurface structure or stratigraphy within or above the Hutchinson Salt Member unique to the Macksville sinkhole could be attributed to its rare catastrophic formation as well as to its preferential growth of formation after initial subsidence.

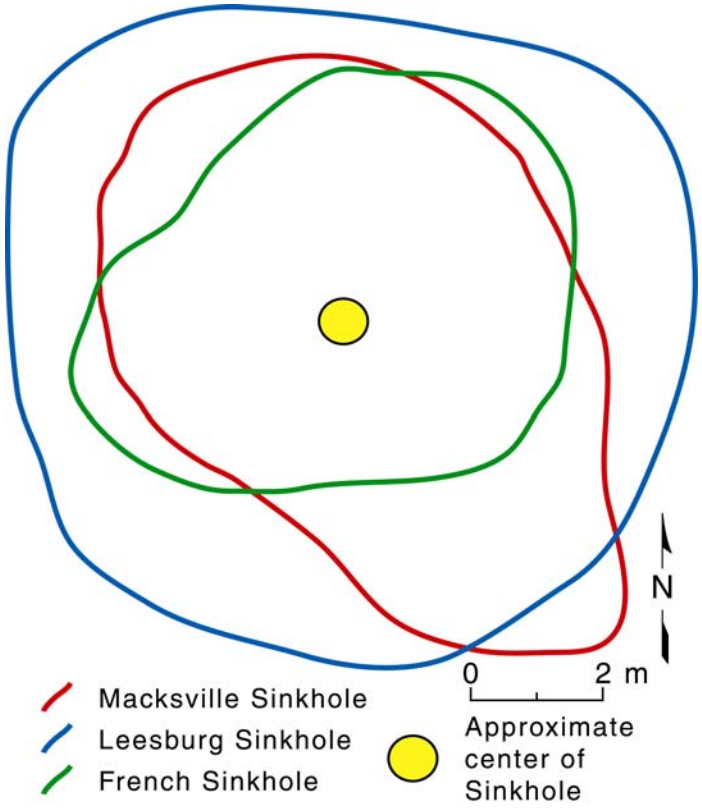

Figure 42: Affected area with approximate centers of sinkholes overlapped visualized using 2002 aerial photos.

Another likely piece of evidence in reconstructing this sinkholes formation is the interpreted two stages of collapse evident on the 1998 north-south seismic line (Figure 30). The initial failure was halted before reaching the ground surface possibly weakened the overburden rock so that the second failure propagated directly to the ground surface. Once a void of sufficient horizontal extent formed in the sediments from salt upward such that roof-rock stress exceeded its strength and failure propagated virtually unimpeded from the void to the ground surface. Water chemistry, hydrostatic head, and unsaturated water volume moving across and through rock influence sinkhole growth. A preferential northeast groundwater gradient in this area complements the preferential dissolution path.

After rock failure migrated upward through all layers between the salt and the ground surface, a multitude of new potential pathways became available for fluid movement. Under the right conditions relatively fresh water immediately above and normally isolated from the Hutchinson Salt Member could have formed a path allowing communication with the salt. Aquifers such as the undifferentiated redbeds from the Permian System, Cheyenne Sandstone, Dakota Formation, Greenhorn Limestone of the Cretaceous System; the Tertiary System (Pliocene Series); the Quaternary system (Pleistocene Series); as well as the Quaternary System (Pleistocene and Recent Series) (McLaughlin, 1949) could gain access to the salt through fractures and faults formed during failure and collapse. This communication will continue to fuel the dissolution process along the ever-expanding pathways.

By building upon earlier investigations of sinkhole development, our understanding of their formation and growth is one step closer to predicting the formation of future subsidence features. Slumping of the overburdened beds was associated with the dissolution of the Hutchinson Salt Member (Knapp et al., 1989). Sinkhole formation is associated to the mechanisms of cavern breakdown (Miller et al., 1997). The Macksville sinkhole brings more insight to the processes than past surveys as well it is consistent with previous studies and builds on out knowledge and confidence. The comparison of the subsurface dissolution to the surface subsidence improves the understanding of sinkhole growth and of the long-term effects that sinkholes can have on human activity or property.

Conclusion

Super-imposing interpretations from the 1998 west-east line onto the 2005 CMP stacked section shows continuing dissolution of the Hutchinson Salt Member. High-resolution time-lapse interpretation of slumping occurring in the Stone Corral Formation and the anhydrites within the Hutchinson Salt Member proved effective at the Macksville sinkhole. Comparing the change in surface subsidence and subsurface dissolution revealed the mathematical confines of the sinkhole.

Interpretations of CMP stacked sections suggest two stages of dissolution. The initial stage occurred as two separate phases. First a void developed and the roof rock failed, but this appears not to have propagated to the ground-surface. In the second phase of dissolution a larger cavity formed that resulted in roof rock failure that propagated rapidly to the surface. This subsidence was followed by a second stage of dissolution with gradual subsidence occurring outside the tensional dome. This can be seen in the deformed overburdened units in the seismic CMP stacked section and the change in elevation on the KCC data.

Key to predicting areas of potential surface subsidence risk is understanding the process responsible for failure, the features controlling failure, and the rate of formation. The Macksville sinkhole initially failed catastrophically but has been gradually subsiding for many years following a logarithmic decline. Investigating changes in the subsurface through time has proven beneficial in attempts to understanding the factors that control the process ($y = Ln(x) + b$). This sinkhole's catastrophic collapse in 1998 is uncommon compared to other sinkholes in Kansas.

Its initial subsidence rate and elongated shape are both out of the ordinary. Therefore, it is a critical data point in unraveling the processes and the characteristics that will some day allow prediction of sinkhole failure rates and extent prior to surface expression. Further investigations are needed to determine an explanation to the elongated shape of the Macksville sinkhole.

References

Allen, K.P., M.L. Johnson, and J.S. May, 1998, High fidelity vibratory seismic (HFVS) method for acquiring seismic data: Society of Exploration Geophysicist [Exp. Abs.], p 140-143.

Anderson, R.Y., and D.W. Kirkland, 1980, Dissolution of salt deposits by brine density flow: Geology, v 8, p 66-69.

ASTM D 7128 - 05, "Standard Guide for using the Seismic-Reflection Method for Shallow Subsurface Investigation," ASTM International.

Baker, G.S., D.W. Steeples, and M. Drake, 1998, Muting the noise cone in near-surface reflection data: An example from southeastern Kansas: Geophysics, v 63, no 4, p 1332-1338.

Beck, B.F., ed., 1984, Sinkholes: their geology, engineering and environmental impact; proceedings of the first multidisciplinary conference on sinkholes: Rotterdam, A.A. Balkema, p 429.

Brittle, K.F., L.R. Lines, and A.K. Dey, 2001, Vibroseis Deconvolution: a comparison of cross-correlation and frequency-domain sweep Deconvolution: Geophysical Prospecting, v 49, p 675-686.

Carmichael, R.S., 1989, Practical Handbook of Physical Properties of Rocks and Minerals: CRC Press, Boca Raton, Fl, p 741.

Carter, N.L., and F.D. Hansen, 1983, Creep of rock salt: Tectonophysics, v 92, p 275-333.

Carüh, C., and J.K. Costain, 1983, Noise attenuation by Vibroseis Whitening (VSW) processing: Geophysics, v 48, no 5, p 543-554.

Davies, W.E., 1951, Mechanics of cavern breakdown: National Speleological Society, v 13, p 6-43.

Doll, W.E., and Carüh, C., 1995, Spectral Whitening of impulsive and swept-source shallow seismic data: Society of Exploration Geophysicist [Exp. Abs.], p 398-401.

Doll, W.E., R.D. Miller, and J. Xia, 1998, A noninvasive shallow seismic source comparison on the Oak Ridge Reservation, Tennessee: Geophysics, v 63, no 4, p 1318-1331.

Ege, J.R., 1984, Formation of solution-subsidence sinkholes above salt beds: U.S. Geological Survey Circular 897, p 1-11.

Ge, H. and M.P.A. Jackson, 1998, Physical Modeling of Structures Formed by Salt Withdrawal: Implications for Deformation Caused by Salt Dissolution: AAPG Bulletin, v 82, n 2, p 228-250.

Goupillaud, P.L., 1976, Signal design in the 'Vibroseis technique': Geophysics, v 41, no 6, p 1291-1304.

Handin, J., 1966,Handbook of Physical Constants: The Geological Society of America, Memoir 97, Sydney P. Clark Jr., ed., p 224-289.

Hunter, J.A., S.E. Pullam, R.A. Burns, R.M. Gagne, and R.L. Good, 1984, Shallow seismic reflection mapping of the overburden-bedrock interface with the engineering seismograph-Some simple techniques: Geophysics, v 49, no 8, p 1381-1385.

Ivanov, J., R.D. Miller, and J. Xia, 1998, High frequency random noise attenuation on shallow seismic reflection data by migration filtering: Society of Exploration Geophysics [Exp. Abs.], p 870-873.

Johnson, K.S., 1986, Salt dissolution and collapse at Winkh sink in west Texas: Columbus, Ohio, Battelle Project Management Division, Office of Nuclear Waste Isolation Technical Report 598, p 79.

Johnson, K.S., 2005, Subsidence hazards due to evaporite dissolution in the United States: Environmental Geologist, v 48, p 395-409.

Jones, O.S., 1945, Disposition of oil-field brines: University of Kansas publications, Lawrence, Kansas.

Klemperer, S.L., 1987, Seismic noise-reduction techniques for use with vertical stacking: An empirical comparison: Geophysics, v 52, no 3, p 322-334.

Knapp, R.W. and D.W. Steeples, 1986a, High-resolution common-depth-point reflection profiling: Instrumentation: Geophysics, v 51, no 2, p 276-282.

Knapp, R.W. and D.W. Steeples, 1986b, High-resolution common-depth-point reflection profiling: Field acquisition parameter design: Geophysics, v 51, no 2, p 283-294.

Knapp, R.W., D.W. Steeples, R.D. Miller, and C.D. McElwee, 1989, Seismic reflection surveys at sinkholes in central Kansas: Geophysics in Kansas, D.W. Steeples, ed., Kansas Geological Survey, Bulletin 226, p 95-116.

Lambrecht, J.L. and R.D. Miller, Catastrophic sinkhole formation in Kansas: A case study: The Leading Edge; in press

Lambrecht, J.L., R.D. Miller, J. Ivanov, and S. Durrant, 2004a, High-resolution seismic imaging of catastrophic salt dissolution sinkhole in central Kansas: Symposium on the Application of Geophysics to Engineering and Environmental Problems [Exp. Abs.], published on CD.

Lambrecht, J.L., R.D. Miller and T.R. Rademacker, 2004b, Advantages and disadvantages of pre-correlation, pre-vertical stack processing on near-surface, high-resolution Vibroseis data: Society of Exploration Geophysicist [Exp. Abs.], p 1425-1428.

Lohmann, H.H., 1972, Salt dissolution in subsurface of British North Sea as interpreted from seismograms: AAPG Bulletin, v 56, p 472-479.

Martinez, J.D., K.S. Johnson, and J.T. Neal, 1998, Sinkholes in evaporite rocks: American Scientist, v 86, p 38-51.

McLaughlin, T.G., 1949, Geology and Ground-water Resources of Pawnee and Edwards Counties, Kansas: Kansas Geological Survey, Bulletin 80.

Merriam, D.F., 1963, The geologic history of Kansas: Kansas Geological Survey, Bulletin 162.

Miller, R.D., 1992, Normal moveout stretch mute on shallow-reflection data: Geophysics, v 57, no 11, p 1502-1507.

Miller, R.D., 2003, High-resolution seismic-reflection investigation of a subsidence feature on U.S. Highway 50 near Hutchinson, Kansas: in K.S. Johnson and J.T. Neal, eds., *Evaporite Karst and Engineering/Environmental Problems in the United States,* Oklahoma Geological Survey, Circular 109, p 157-167.

Miller, R.D. and D.W. Steeples, 1991, Seismic-Reflection processing demonstration using Eavesdropper: The Kansas Geological Survey, Open-file Report 91-27.

Miller, R.D., D.W. Steeples, P.B. Myers, and D. Somanas, 1988, Seismic reflection surveys at the Knackstedt salt-water disposal well: Kansas Geological Survey, Open-file Report 88-31.

Miller, R.D., D.W. Steeples, L. Schulte, and J. Davenport, 1993, Shallow seismic reflection study of a salt dissolution well field neat Hutchinson, Kansas: Mining Engineering, October, p. 1291-1296.

Miller, R.D., D.W. Steeples, and T.V. Weis, 1995, Shallow seismic-reflection study of a salt-dissolution subsidence feature in Stafford County, Kansas: in N.L. Anderson and D.E. Hedke, eds., Geophysical Atlas of Selected Oil and Gas Fields in Kansas: Kansas Geological Survey Bulletin, 237, p 71-76.

Miller, R.D., D.W. Steeples, F.T. Wirnkar, and D.A. Keiswetter, 1990, Shallow seismic-reflection study of the Siefkes salt dissolution sinkhole in Stafford County for Quinoco Petroleum: Kansas Geological Survey, Open-file Report 90-32.

Miller, R.D., A.C. Villella, J. Xia, 1997, Shallow high-resolution seismic reflection to delineate upper 400 m around a collapse feature in central Kansas: Environmental Geosciences, v 4, no 3, p 119-126.

Miller, R.D., A. Villella, J. Xia, and D.W. Steeples, Seismic investigation of a salt dissolution feature in Kansas: Special Publication: Near-Surface Geophysics, Volume II, Society of Exploration Geophysicists, in press.

Miller, R.D. and J. Xia, 2002, High-resolution seismic reflection investigation of a subsidence feature on US highway 50 near Hutchinson, Kansas: Symposium on the Application of Geophysics to Engineering and Environmental Problems [Exp. Abs.], published on CD.

Nieto, A.S., D. Stump, and D.G. Russel, 1985, A mechanism for sinkhole development above brine cavities in the Windsor-Detroit area, in B.C. Schreiber and H.L. Harner, eds., Sixth international symposium on salt: Alexandria, Virginia, The Salt Institute, V 1, p 351-367.

Parker, J.M., 1967, Salt solution and subsidence structures, Wyoming, north Dakota, and Montana: AAPG Bulletin, v 51, p 1929-1947.

Salt Institute, 2003, Major salt deposits and dry salt production in North America: Salt Institute, Alexandria, Virginia.

Samuel, W.G. and S.M. Trader, 2002, The mechanism of sinkhole formation in glacial sediments above the Retsof Salt Mine: Evaporite Karst and Engineering and Environmental Problems in the United States, [Abs.], http://gsa.confex.com/gsa/2002AM/finalprogram/abstract_38767.htm

Sheriff, R.E., 2002, Encyclopedic Dictionary of Exploration Geophysics: Society of Exploration Geophysicists, Tulsa, Oklahoma.

Steeples, D.W., 1980, Seismic reflection investigations of sinkholes in Russell and Ellis counties, Kansas: Progress report to the Kansas Department of Health and Environment and the Kansas Department of Transportation.

Steeples, D.W. and R.W. Knapp, 1982, Seismic investigation of sinkholes in Russell and Ellis counties, Kansas: Final report to the Kansas Department of Health and Environment.

Steeples, D.W., R.W. Knapp, and C.D. McElwee, 1983, Seismic reflection surveys of a catastrophically collapsed sinkhole, Ellis County, Kansas: Society of Exploration Geophysicist [Exp. Abs.], p 296-298.

Steeples, D.W., R.W. Knapp, and C.D. McElwee, 1986, Seismic Reflection investigation of sinkholes beneath interstate highway 70 in Kansas: Geophysics, v 51, no 2, p 295-301.

Steeples, D.W. and R.D. Miller, 1990, Seismic reflection methods applied to engineering, environmental, and groundwater problems: Society of Exploration Geophysics, Geotechnical and Environmental Geophysics, Stan Ward, ed., Vol. 1: Review and tutorial, p 1-30.

Villella, A.C., 1998, Seismic investigation of a salt dissolution feature in Kansas: Thesis (M.S.), University of Kansas.

Walters, R.F., 1978, Land subsidence in central Kansas related to salt dissolution: Kansas Geological Survey, Bulletin 214.

Walters, R.F., 1991, Gorham Oil Field: Kansas Geological Survey, Bulletin 228.

Whatney, W.L., J.A. Berg, and S. Paul, 1988, Origin and distribution for the Hutchinson Salt (lower Leonardian) in Kansas: Midcontinent SEPM Special Publication no. 1, p 113-135.

White, W.B., 1988, Geomorphology and hydrology of karst terrains: Oxford University Press.

Whittemore, D.O., 1989, Geochemical characterization of saltwater contamination in the Macksville sink and adjacent aquifer: Kansas Geological Survey, Open-file Report 89-35.

Widess, M.B., 1973, How thin is a thin bed?: Geophysics, v 38, p 1176-1180.

Yilmaz, O., 2001, Investigations in Geophysics no. 10: Seismic data Analysis: Society of Exploration Geophysicists, Tulsa, Oklahoma.

Zeller, D.E., 1968, The stratigraphic succession in Kansas: Kansas Geological Survey Bulletin 189.